8-2015

Histone H3 K4 methylation regulates the Spindle Assembly Checkpoint through direct binding of multiple checkpoint components and Cdc20

Andria C. Schibler

Histone H3 K4 methylation regulates the Spindle Assembly Checkpoint through direct binding of multiple checkpoint components and Cdc20

BY

Andria Schibler, Ph.D. Candidate

APPROVED:

_____

Sharon Y.R. Dent, Ph.D., Supervisory Professor

_____

Mark T. Bedford, Ph.D.

_____

Jill Schumacher, Ph.D.

_____

Xiaobing Shi, Ph.D.

_____

Xuetong Shen, Ph.D.

APPROVED:

_____

Dean of The University of Texas Graduate School of Biomedical Sciences at Houston

Histone H3 K4 methylation regulates the Spindle Assembly Checkpoint through direct binding of multiple checkpoint components and Cdc20

A

Dissertation

Presented to the Faculty of

The University of Texas Health Science Center at Houston

And

The University of Texas M.D. Anderson Cancer Center

Graduate School of Biomedical Sciences

in Partial Fulfillment

of the Requirements

for the degree of

DOCTOR OF PHILOSOPHY

By

Andria Schibler, Ph.D. Candidate

Houston, Texas

August 2015

Dedication

This thesis is dedicated to the businesses, taxpayers, and government funding agencies which financed my education and research.

Acknowledgements

First, I would like to express my sincerest gratitude to the residents of Texas for supporting my research and education. Without the establishment of the MD Anderson and the funding of CPRIT I would not have had such great research and educational opportunities. By attending graduate school in Texas, I was given access to mentors, facilities, equipment, and reagents that most scientists only can dream of. In addition, members of the community took it upon themselves to privately fund and support graduate student research. With that, I would like to thank the Schissler family. The Schissler family funds multiple fellowships for graduate students, which have been instrumental for our success at a time when our education and careers are most vulnerable. Lastly I would like to thank the Sowell and Wade families for their generous fundraising, donations, and scholarship. Texas maintains extremely charitable communities and the support given to the hospitals, education, and research community is outstanding.

I would also like to thank my committee members Dr. Pierre McCrea, Dr. Shelley Sazer, Dr. Kevin Morano, Dr. Jill Schumacher, Dr. Xiaobing Shi, Dr. Snow Shen, and Dr. Mark Bedford for their support and advice, with special thanks to Dr. Jill Schumacher for the additional encouragement. I would also like to thank Dr. Khandan Keyomarsi and Dr. Stephanie Watowich. With their support in the final stages of graduate school, I was able to finalize my research project, which put me in a great position to advance my career.

I wish to also acknowledge the fellow students who I started graduate school with and developed irreplaceable friendships. With that, Akanksha Singh has always been a great friend, supportive, open minded, and one of the most ethical persons I have ever met. Sara Gorjestani is the most considerate, compassionate and understanding of us all. Douglas Caruthers has the kindest heart. Deepavali Chakravarti is the most savvy and generous. Lastly, Lorena Mali was the most welcoming and open; she showed me an underground Houston culture that I could have only dreamed about. Graduate school was worthwhile even if I only obtained the friendships.

I would like to thank past and present lab members especially Li Wang for her never to be forgotten unselfishness. I would like to thank Dr. Evangelia (Liah) Koutelou for the help and encouragement, I cannot express how much she has done for me and I would not be where I am today without her. In addition, I would like to thank Dr. Junya Tomida. He is honestly one of the most talented and well-trained scientists I have ever had the pleasure to work with. I am extremely grateful to have Junya as a collaborator and I would not have learned nearly as many experimental procedures if he was not so generous. Both Liah and Junya are influential to my current and future scientific success.

Lastly, I would like to thank Dr. Sharon Dent. Sharon combines a classic demeanor and charm with intelligence, awareness, and sensibilities that are fiercely ahead of our time. She is and will always be three steps ahead scientifically, socially, and professionally. Sharon is also remarkably unique, adaptable, and talented. I can say that after 8 years in her lab, I have yet to be disappointed either personally or professionally. Because of

this, her impressiveness, and multiple achievements she is one of the only persons I have ever looked up to. She is a great role model for any young scientist and I was extremely fortunate to work in her lab.

Histone H3 K4 methylation regulates the Spindle Assembly Checkpoint through direct binding of multiple checkpoint components and Cdc20

Andria Schibler, Ph.D. Candidate

Supervisory Professor: Sharon Dent, Ph.D.

Histone H3K4 methylation is conserved across species and is associated with active transcription. By using *Saccharomyces cerevisiae*, we found histone H3K4 methylation has a previously unknown role in regulating mitosis through the Spindle Assembly Checkpoint. The Spindle Assembly Checkpoint ensures duplicated chromosomes are segregated correctly and each daughter cell receives one full copy of the genome. Our data show *SET1* mutants and histone H3K4 mutants display a resistance to the mitotic poison, benomyl. Moreover methylated histone H3 directly binds to Spindle Assembly Checkpoint proteins Bub3 and Mad2 as well as the activator of the Anaphase Promoting Complex (APC) protein Cdc20. *MAD2* encodes a HORMA domain, which I identify as a novel histone binding motif. Mad2 maintains two differing conformations, closed Mad2 (C-Mad2) and open Mad2 (O-Mad2). We find C-Mad2 increases the Mad2-H3 interaction. In addition, O-Mad2 limits the H3-Mad2 interaction. Further analysis, shows C-Mad2 can bind to all unmodified, mono-, di-, and tri-methylated H3K4 while O-Mad2 loses H3 binding ability when H3K4 is di- or tri-methylated. Here we show H3K4 methylation inhibits the Spindle Assembly Checkpoint from correctly deactivating after cell cycle arrest by binding C-Mad2.

Table of Contents

List of Figures and Tables

Chapter 1: Introduction

Chromatin during DNA Replication, Transcription and Repair

The eukaryotic genome is made up DNA, which is wrapped around histone proteins to form nucleosomes. Each canonical nucleosome contains two copies of histone H2A, H2B, H3 and H4 and 146 bp of DNA. Multiple nucleosomes further condense into chromatin fibers in a highly ordered manner, which constitute chromosomes. Although the genome is tightly wrapped around nucleosomes, genomic DNA must be accessible for cellular functions such as DNA replication, transcription, and DNA repair.

Replication

Before division can occur, cells must first duplicate each chromosome. *Saccharomyces cerevisiae* is used as a model to better understand the DNA elements and proteins required for DNA replication. By using genetic screens in *S. cerevisiae*, it was found DNA synthesis requires Autonomously Replicating Sequence (ARS) elements, which recruit proteins essential for DNA replication. The ARS is the location at which multiple proteins associate and form the pre-replication complex (pre-RC) in a stepwise fashion. First, the Origin Recognition Complex (ORC) identifies and binds the ARS Consensus Sequence (ACS) and recruits Cdc6 and Cdt1. The ORC, Cdc6 and Cdt1 subsequently recruit the MCM (Mini Chromosome Maintenance) complex. Once all of these components are assembled replication can begin and chromosomes can be duplicated.

Nucleosome occupancy must be highly coordinated to concur with DNA replication. For replication to take place, the ACS must be free from nucleosomes to promote ORC recognition and binding (Simpson, 1990). Nucleosomes must be limited, removed, or repositioned from the ACS to create the nucleosome free region (NFR). Surprisingly, nucleosomes proximal to the ACS are required for the pre-RC formation (Lipford and Bell, 2001), implicating nucleosome positioning as an intricate regulatory step necessary for proper DNA replication. Before new genomic DNA can be polymerized, nucleosomes must be removed and after DNA synthesis, histone octamers must be deposited and reassembled onto DNA creating two sister chromatids. This temporal and spatial regulation process is coordinated by linking the MCM complex with histone chaperone proteins with a physical association between DNA duplication machinery and proteins able to remove and reassemble nucleosomes (Groth et al., 2007).

Transcription

Comparable to how DNA polymerases need NFRs to function during replication, RNA polymerases also require access to DNA during transcription. Therefore, transcription is a DNA-based cellular process, which is either inhibited or promoted through nucleosome positioning and remodeling. The gene promoter, a region upstream of the gene body, that dictates where RNA polymerase will bind, thereby defining the transcription start site (TSS), is critical to facilitate transcription. Gene promoters and sequence specific binding sites for transcription factors correlate with NFRs (Bernstein et al., 2004; Lee et al., 2007b; Yuan et al., 2005) allowing access to the genome. In

addition, NFRs are associated with the region past the gene body after the transcription termination site (TTS) (Mavrich et al., 2008). Lastly, throughout the gene body, there is a high occupancy of nucleosomes, suggesting the gene regulatory regions are accessible and the coding regions are protected. This allows for regulatory proteins to bind and recruit transcriptional elements, although the nucleosomes must be moved or evicted prior to RNA synthesis and reassembled or replaced after the gene body has been transcribed into mRNA. Regulatory complexes such as ATP-dependent chromatin remodelers and the regulation of histone occupancy by transcription factors is one way of controlling the access to DNA for mRNA generation. For example, loss of function mutations of the DNA binding proteins that promote transcription, such as Abf1, Reb1, and Rap1, showed an increase in nucleosome occupancy suggesting active transcription can also affect nucleosome positioning and DNA accessibility (Badis et al., 2008; Ganapathi et al., 2011).

In addition, ATP dependent chromatin remodelers can either evict or move nucleosomes. Two well studied chromatin remodeling complexes that were found to remove nucleosomes and regulate transcription are the SWI/SNF complex and the RSC complex. The SWI/SNF complex was shown to remove nucleosomes and this eviction subsequently regulates transcription (Hirschhorn et al., 1992; Matallana et al., 1992). Unlike the SWI/SNF complex, which is exclusively recruited to RNA PolII genes, another chromatin remodeling complex was shown to regulate both RNA PolII

and PolIII transcription. The RSC complex was shown to remodel chromatin as well as regulate transcription (Cairns et al., 1996).

DNA Repair

DNA damage must be repaired to maintain genomic integrity and support cell survival. Exposure to UV radiation induces DNA lesions, which must be identified and remedied through nucleotide excision repair (NER). Although most UV lesions take place within DNA wrapped around the histone octamer (Gale et al., 1987), the nucleosome must be removed or evicted prior to DNA damage repair. Previous studies reported nucleosomal remodeling after UV induced DNA damage and repair (Smerdon and Lieberman, 1978) indicating a cellular response to reposition nucleosomes and facilitate access to the damaged DNA. Further studies identified Rad4 and Rad23 as proteins required for the identification of DNA lesions (Jansen et al., 1998) and additional research found the SWI/SNF chromatin remodeling complex induced nucleosomal changes upon UV damage (Yu et al., 2005). Lastly, it has been reported that subunits of the SWI/SNF complex purify with Rad4 and this interaction was enhanced upon UV irradiation treatment, linking the identification of DNA lesions with the recruitment of chromatin remodeling complexes to facilitate NER (Gong et al., 2006).

Double strand breaks are an additional deleterious DNA damaging event and can be repaired by two differing pathways homologous recombination (HR) and

nonhomologous end-joining (NHEJ). NHEJ requires Ku70 and Ku80, which bind to DNA and the DNA ligase IV factors Lif1 and Nje1 in combination with the catalytic subunit Dnl4 to properly repair DSBs (Varambally et al., 2005). HR requires Rad50, Mre11, and Xrs2 proteins, which compose the Mre11 complex. The Mre11 complex can bind to DNA and exhibits exonuclease activity (Chen et al., 2001; Paull and Gellert, 1998) required for DSB repair through HR. Interestingly, chromatin remodeling complexes have also been implicated in DSB repair. Both INO80 and the SWI/SNF complexes have been localized to sites of DSBs by chromatin immunoprecipitation (ChIP) experiments and mutations to these complexes result in a sensitivity to DNA damaging agents (Chai et al., 2005; van Attikum et al., 2004). The INO80 complex was later shown to remove histones from sites of DSBs and disruption of this event resulted in a loss of efficient binding of the Mre11 complex (van Attikum et al., 2007) indicating a requirement for nucleosome remodeling prior to DSB repair.

Histones and Histone modifications

In addition to nucleosome remodeling, chromatin is regulated through post-translational modifications (PTMs). Histone proteins contain an unstructured N-terminal tail that protrudes from the “core” portion of the nucleosome (Luger et al., 1997). Histone tails are subjected to covalent PTMs such as acetylation, phosphorylation, ubiquitination, and methylation among others (Strahl and Allis, 2000). Histone modifications are known to alter chromatin structure and selectively recruit or exclude protein complexes and other histone modifying enzymes to histones thus regulating many cellular

processes such as DNA damage (Sollier et al., 2004), transcription (Santos-Rosa et al., 2002), and telomere maintenance (Krogan et al., 2002). Histone modifications are found on all histones, including the canonical histones, H2A, H2B, H3, and H4. Lastly, histone modifications and their downstream functions are highly conserved from yeast to human.

In addition to the nucleosome remodeling required for proper DNA replication and repair, PTMs of histone tails are also implicated in regulating these processes. A number of mutations affecting histone PTMs result in inefficient DNA replication suggesting loss of specific histone modifications affect DNA duplication. Histone modifications such as H3 and H4 acetylation, H3K36 methylation, and H3K4 methylation (Pryde et al., 2009; Rizzardi et al., 2012; Unnikrishnan et al., 2010) Lastly, mutants inhibiting specific PTMs of histone tails, such as H2A phosphorylation, H2B ubiquitination, H3K79 methylation as well as multiple actetylation events on H3 and H4 are sensitive to ionizing radiation exposure, which is a DNA damaging agent resulting in DSBs (reviewed in (Li, 2012).

PTMs of histones have been extensively studied during transcription with specific histone modifications concurring with transcription activation, while other histone modifications are associated with a silenced or inactive chromatin status. Histone acetylation has been largely studied as an active transcriptional mark because this modification can interrupt the association of the histone octamer with DNA. Gcn5 is a

well-studied histone acetyltransferase with activity towards lysines on H2B, H3, and H4 (Suka et al., 2001; Winkler et al., 2002). Although, histone methylation can take place on both arginines and lysines, lysine methylation of Histone H3K4 and K36 are associated with active transcription in yeast (Bernstein et al., 2002; Rao et al., 2005).

Histone H3 Methylation

In yeast, histone H3 K4, K36, and K79 can be mono-, di-, or tri-methylated (Garcia et al., 2007) and these methylation events have specific roles and are positioned precisely. In particular, Histone H3K4 trimethylation localizes to gene promoters and is associated with active transcription. In addition, H3K4 dimethylation is located throughout the gene body of both repressed and active genes (Bernstein et al., 2002; Santos-Rosa et al., 2002). Histone H3K4 methylation has been extensively studied in multiple organisms. Histone H3K4 methylation is associated with active transcription in yeast and this is conserved in mammals (Bernstein et al., 2002) (Krogan et al., 2003). In addition, H3K4 methylation is enriched at replication origins and loss of H3K4 dimethylation affects replication efficiency (Rizzardi et al., 2012). Unlike humans, which maintain multiple H3K4 methyltransferases, such as SET1A, SET1B, MLL1, MLL2, MLL3 and MLL4, yeast Set1 is responsible for all H3K4 methylation events (Shilatifard, 2012). Removing or inhibiting *SET1* in yeast results in a loss of all detectable histone H3K4 methylation events.

The enzymes required for each lysine methyltransferase event on histone H3 has been

identified. The lysine methyltransferase responsible for H3K36 methylation is Set2 and the protein that methylates histone H3K79 is Dot1. Lastly the H3K4 methyltransferase is Set1. Set1 resides inside a multiprotein complex termed COMPASS. The COMPASS complex is well-studied and exhibits lysine methyltransferase activity when Set1, the catalytic subunit is included. Once incorporated into COMPASS, Set1 can mono-, di-, and tri-methylated histone H3K4. In yeast, multiple components of COMPASS have been identified through biochemical purification, including Swd1, Swd2, Swd3, Spp1, Bre2, Set1, Sdc1, and Shg1 (Figure 1) (Miller et al., 2001).

Yeast Set1 is a conserved protein with homology to human MLL1. In humans, translocations of MLL1 are associated with leukemogenesis (Zeleznik-Le et al., 1994) and correlates with a poor prognosis (Pui et al., 1994). Interestingly, the Set1 complex and the MLL complex maintain strikingly similar features. Set1 requires incorporation into COMPASS for lysine methylation activity, while MLL is also incorporated into a COMPASS-like complex. Presently, little is known about how mutating *MLL1* contributes to leukemogenesis. Selecting known cellular functions regulated by *SET1* in yeast will identify unknown pathways regulated by *MLL1* in humans.

Regulation of H3K4 methylation

H3K4 methylation is highly regulated. Multiple cellular events are required for H3K4 methylation. Previous research found H2B mono-ubiquitination is necessary for di- and trimethylation of histone H3K4 (Sun and Allis, 2002). In yeast, histone H2B is mono-

ubiquitinated on lysine (K) 123 and this is conserved on K120 in vertebrates (Thorne et al., 1987). The E2 enzyme, Rad6, required for this modification has been identified (Robzyk et al., 2000). Later studies found Bre1, an E3 ligase, is also required (Wood et al., 2003) for H2B ubiquitination, and loss of either Rad6 or Bre1 abolishes detectable H3 K4 di- and trimethylation although H3K4 monomethylation is still present (Seol et al., 2006). Additional studies identified H2B ubiquitination is also an upstream event for dimethylation and trimethylation of histone K79 but not mono-methylation of this lysine residue. Interestingly, although histone H3K4 and K79 methylation are events associated with active transcription, another active mark, histone H3K36 methylation, was not affected (Dehe et al., 2005; Shahbazian et al., 2005).

Methyl Reading Domains

A main function of histone H3 methylation is to either promote or inhibit protein-protein interactions. Fitting with this model, a number of lysine methyl binding motifs have been identified. One example is the WD40 domain, which was shown to read differing H3K4 methylation states (Wysocka et al., 2005). An additional protein with the ability to read H3K4me2 is PHF20, which contains a Tudor domain (Kim et al., 2006). Also, proteins containing PHD fingers were identified as methyl readers. More specifically the PHD finger of ING2 was shown to preferentially bind H3K4me3 (Shi et al., 2006). Lastly, chromo, MBT, and PWWP domains have been shown to selectively interact with distinct H3 methylation events (Bannister et al., 2001; Kim et al., 2006; Wang et al., 2009).

Figure 1: The COMPASS Complex

An illustration of the multi-protein complex termed COMPASS. COMPASS is composed of multiple proteins including Swd1, Swd2, Swd3, Bre2, Sdc1, Spp1, Shg1, and the catalytic subunit, Set1.

Figure 1

Non-histone substrates of COMPASS

In addition to methylation of histone H3, COMPASS can also dimethylate Dam1, which is a kinetochore protein associated with the DASH complex. In yeast, the DASH complex forms a ring around microtubules and localizes to the kinetochore during cellular division. Dam1 methylation events block Ipl1 mediated phosphorylation of surrounding serines (Zhang et al., 2005). The regulatory events required for Dam1 methylation have bee identified. Like H3K4 methylation Dam1 methylation requires H2B ubiquitination, which shows changes in chromatin modifications can also affect the PTMs of non-histone proteins (Latham et al., 2011).

Cell Division

Cell division is a multi-step process that involves the partitioning of the newly duplicated genome into two daughter cells. Prior to mitosis the genome must be replicated which requires the removal of nucleosomes and repackaging of the sister chromatids into newly duplicated chromosomes. During mitosis, DNA must segregate evenly allowing for one complete copy of each genome to be maintained in each newly formed cell. *S. cerevisiae* divides the duplicated genome by connecting the mitotic spindle to each duplicated chromosome, or sister chromatid, in a bipolar fashion via the kinetochore. The kinetochore is a multi-protein complex associated with the centromeric region of each sister chromatid. These microtubule-kinetochore attachments allow for tension across the mitotic spindle from one spindle pole body to the other. The sister chromatids are then pulled away from each other to opposite sides of the cell before

the two nuclei segregate and the daughter cells divide. Ipl1 is the sole Aurora kinase in yeast and regulates many mitotic functions during cellular division. Ipl1 mediated phosphorylation events regulate microtubule-kinetochore interactions and mitotic spindle disassembly (Biggins et al., 1999; Buvelot et al., 2003).

The Spindle Assembly Checkpoint

To guard against aberrant chromosome segregation during cell division, eukaryotes maintain the Spindle Assembly Checkpoint (SAC), which acts as a surveillance mechanism to identify defects in tension (Li and Nicklas, 1995) or mitotic spindle-kinetochore attachments (Rieder et al., 1994). Thus, the SAC pathway ensures each cell maintains one complete copy of the genome.

If improper microtubule-kinetochore attachments or lack of tension across the mitotic spindle arise during mitosis, Ipl1 phosphorylates a number of kinetochore proteins which activate the SAC preventing the cell from entering anaphase until these defects are remedied (Biggins and Murray, 2001). Loss of SAC function results in aneuploidy, a hallmark of cancer, therefore the SAC is essential for maintaining genomic integrity. Previous studies used *S. cerevisiae* as a model to identify components of the SAC such as *MAD1* (Mitotic Arrest Defect 1), *MAD2*, *MAD3* (Li and Murray, 1991) *BUB1* (Budding Uninhibited by Benomyl 1) and *BUB3* (Hoyt et al., 1991) among others. Mutations in these genes prevent activation of the SAC, resulting in aneuploidy. These mutants are also sensitive to mitotic poisons that stress the cell during mitosis, such as

benomyl and nocodazole. Benomyl and nocodazole destabilize mitotic spindle microtubules thereby interrupting proper mitotic spindle-kinetochore interactions creating a loss of tension. Stressing mutant cells with mitotic poisons antagonizes mitotic spindle polymerization and chromosome attachments causing the Spindle Assembly Checkpoint to be engaged and evaluated. In mutants defective in SAC activation, chromosomes divide without a surveillance mechanism to assess proper mitotic spindle-kinetochore attachments and tension, thereby subjecting cells to an increased risk of aneuploidy and eventual cell death.

By using genetic and molecular techniques the SAC has been extensively studied. Previous research found that the SAC is spatially and temporally regulated. Until SAC activation, Mad1 and Mad2 localize to the nuclear pore complex (Iouk et al., 2002). Bub1 and Bub3 bind to kinetochores in early mitosis regardless of a mitotic disturbance. In contrast, Mad1 and Mad2 localize to the kinetochore only following SAC activation (Gillett et al., 2004). SAC components not only localize to the kinetochore for mitotic regulation, SAC proteins bind to and inhibit Cdc20. Cdc20 is a component of the Anaphase Promoting Complex (APC) and Cdc20 is thought to recruit proteins to the APC for ubiquitination and subsequent protein degradation. SAC inhibition of the APC through Cdc20 is due to Bub3, Mad2, and Mad3 directly binding Cdc20 (Figure 2), which causes APC inhibition, decreased proteolysis, and increased stability of a number of APC substrates such as Pds1 (Securin), Ase1, and Clb2.

After SAC activation, Mad2 binds to Cdc20 and adopts a specific active closed Mad2 (C-Mad2) conformation, while free Mad2 remains in an inactive open Mad2 (O-Mad2) conformation (Luo et al., 2000; Nezi et al., 2006; Sironi et al., 2002). The C-Mad2-Cdc20 complex is thought to create a template that converts O-Mad2 to C-Mad2 for further inhibition of Cdc20, thereby perpetuating SAC activation, cell cycle arrest, and APC inhibition. The formation of the O-Mad2-C-Mad2 dimer is required for proper SAC activation and mitotic arrest in yeast (Nezi et al., 2006). Although much is known about how the SAC is activated and maintained, few experiments show how the SAC is silenced. In vertebrates, $p31^{comet}$ was shown to be a negative regulator of the SAC (Xia et al., 2004). $p31^{comet}$ interacts directly with C-Mad2 but can not bind to O-Mad2. Moreover, binding of $p31^{comet}$ to C-Mad2 blocks C-Mad2-O-Mad2 dimerization, thereby preventing Cdc20 inhibition effectively silencing the SAC (Habu et al., 2002; Mapelli et al., 2006; Xia et al., 2004).

Histone modifications are known to alter chromatin structure and selectively recruit or exclude protein complexes to histones thus regulating many cellular processes. In this study, we examined COMPASS and the role of histone H3 K4 methylation in regulating mitosis. Here we demonstrate that Set1, a lysine methyltransferase negatively regulates the SAC through methylation of histone H3K4.

Figure 2: An Illustration of APC inhibition by SAC proteins

Cdc20 is an activator of the Anaphase Promoting Complex (APC) and Cdc20 recruits substrates to the APC for subsequent lysine ubiquitination and proteolysis (active). The SAC components Bub3, Mad2, and Mad3 bind to Cdc20 and inhibit the E3 ligase activity of the APC (inactive).

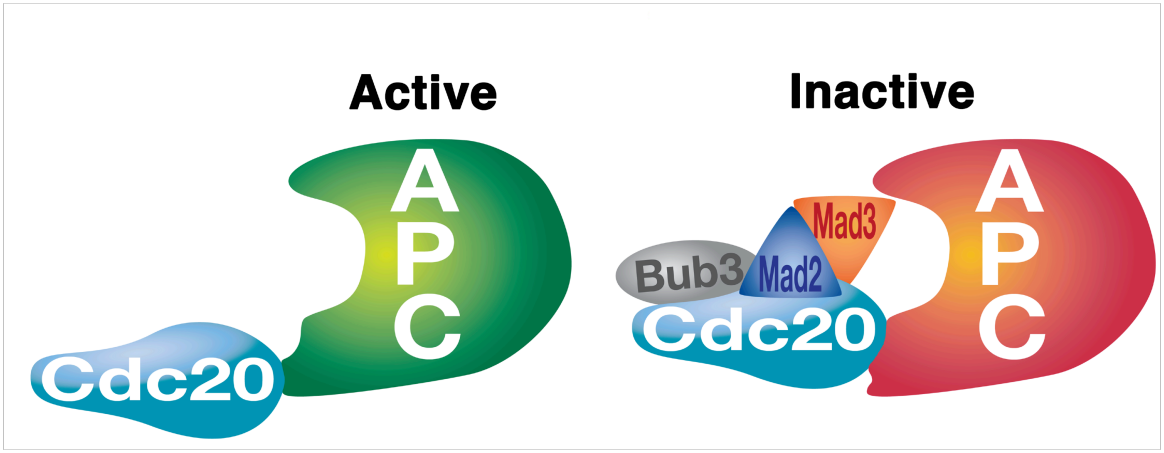

Figure 2

Aims and Rationale for This Study

The cellular role of Ipl1 (Increase in Ploidy 1) has been extensively studied, and previous research determined that Ipl1 functions in regulating mitosis through phosphorylation of a number of kinetochore substrates (Cheeseman et al., 2002). *IPL1* temperature sensitive mutants lose and gain chromosomes due to a decrease in phosphorylation in kinetochore components. Previous research determined that a catalytically inactive *set1* mutant has the ability to suppress the temperature sensitivity phenotype of mutant *IPL1*, showing Set1 regulates mitotic processes through lysine methylation. In addition, *IPL1* mutant temperature sensitivity could be rescued by limiting the methylation of a novel Set1 substrate and kinetochore protein, Dam1. These data show not only that Set1 has mitotic functions, that include methylation events that take place at the kinetochore (Zhang et al., 2005). These data and others show Set1 has the ability to regulate mitosis through lysine methylation of non-histone substrates. In this study, we further investigated how Set1 regulates mitosis through lysine methylation activity with the following specific aims:

1) **Define how Set1 regulates mitosis or mitotic checkpoints through lysine methylation of Set1 substrates.** Previous lab members identified Set1 regulates mitosis through a novel Dam1 methylation event that takes place at the kinetochore. I will further define how lysine methylation regulates mitosis by using genetic mutants

that abolish total all methylation of Set1 substrates as well as mutants that abolish individual methylation events of Set1 substrates such as histone H3 and Dam1.

2) **Define cell cycle changes and molecular events associated with loss of Set1 mediated lysine methylation.** Molecular studies such as Chromatin Immunoprecipitation (ChIP) assays, confocal microscopy, and cell cycle arrest and release experiments have uncovered numerous cellular events regulated by Ipl1. Because Set1 is known to attenuate the function of Ipl1 through lysine methylation, we will use similar assays with wild-type and *set1* mutant cells to assay cell cycle changes, protein localization, and cell cycle phenotypes in cells deficient for Set1 mediated lysine methylation.
3) **Identify binding partners that interact with methylated and unmethylated Set1 substrates.** A major function of lysine methylation is to regulate protein-protein interactions. Although many methyl-lysine dependent binding proteins involved in transcriptional regulation have been defined, none have been identified during mitosis. I will perform *in vitro* experiments with recombinant proteins, to identify novel histone H3 or Dam1 binding events. In the future, I will compare this binding in both wild-type and *set1* mutants *in vivo*. Identifying proteins that are recruited to or excluded by methylated lysines in response to cell cycle checkpoints or mitosis will elucidate the mechanism by which Set1 regulates cell division.

Chapter 2: Materials and Methods

Yeast Strain Generation, Media, and Culture Conditions

Strains were derived from the BY4741 background using standard techniques (Burke et al., 2000). All strains generated in this study are isogenic to the wild-type strain unless otherwise noted. Deletion strains were constructed by replacing endogenous genes with a one-step gene replacement strategy. Cells were transformed and placed onto selection media to isolate resistant colonies. Genomic DNA was isolated from individual colonies and proper integration was verified by PCR using one primer specific to the cassette and one primer downstream of the gene locus. Strains used in this study are listed in Table 1 and primers used to generate or genotype these strains are listed in Table 2. All strains were grown in YPD (Yeast Peptone Dextrose) complete media at 30^0 C and collected at mid-log phase for analysis unless otherwise noted.

Benomyl Resistance Assays

Plates were prepared with the indicated amounts of benomyl, dissolved in dimethyl sulfoxide (DMSO). Wild-type and mutant strains were grown overnight in rich media and placed onto either control plates (YPD or YPD with DMSO) or YPD plates containing benomyl (10μg/mL, 20μg/mL, 30μg/mL, and 40μg/mL). Plates were placed for 2-3 days at 30^0 C unless stated otherwise.

Cell cycle distribution analysis

Asynchronous mid-log phase cells were pelleted and resuspended in 4% paraformladahyde for 30 minutes, washed 3 times with PBS, and mounted onto slides. Cells were visualized by taking DIC images. The budding index of wild-type and *set1* mutants were assessed by dividing cells into three categories; cells with no bud, cells with a small bud, and cells with a large bud. These categories correspond to G1, S, and G2/M, respectively.

Flow cytometry

5mL culture of mid-log phase cells were pelleted and resuspended in 3 mL of dH_2O. 7 mL of 95% ethanol was added to the culture and incubated overnight at 4^0 C. Cells were pelleted washed in 5mL sodium citrate (pH 7.4). Cells are pelleted again and resuspended in 1mL 50mM sodium citrate with 0.25 mg/mL RNAse, and incubated for 1 hour at 50^0 C. Proteinase K is then added for a final concentration of 1mg/mL and incubated for an additional hour at 50^0 C. 1mL of sodium citrate containing 16mg/mL of propidium iodide was added for a final concentration of 8mg/mL and incubated for 30 minutes before flow cytometry analysis. Data was collected on a BD LSRFortessa™ (Becton Dickinson, San Jose, CA) and analyzed using FlowJo 7.6 software. Protocol was courtesy of Stephen P. Bell and can be found at: http://web.mit.edu/flowcytometry/www/.

Light Microscopy, DIC Images, and Budding Index

Yeast strains were pelleted and resuspended in 4% paraformladahyde for 30 minutes, washed 3 times with PBS, and imaged. DIC images were taken on a Nikon 80i upright microscope using a Plan Apo 60x/1.4 N.A. objective. The microscope is controlled by Nikon Elements AR software. DIC images were used to calculate a budding index for each strain and assess overall cellular morphology.

Immunofluorescence

Immunofluorescence experiments were performed according to standard techniques (Burke et al., 2000). To visualize the mitotic spindle and nuclei, we used an anti-tubulin antibody (Millipore, CBL270, 1:500) and DAPI (Molecular Probes, 1μM). Following staining procedures, images of wild-type and mutant yeast cells were acquired with a LSM510-Meta confocal microscope (Carl Zeiss, Germany) using a 100× PlanApochromat/1.4 N.A. objective**.** Images were processed using ImageJ software (NIH) and Adobe Photoshop.

Recombinant Protein Generation and Purification

Budding yeast SAC genes were cloned into a pGEX4T1 vector to generate a N-terminally tagged GST fusion protein (a description of the plasmids generated can be found in Table 3). Mutations were generated by using the QuikChange XL kit (Stratagene) and sequenced. Proteins were expressed in the *Escherichia coli* strain Rosetta 2 (Novagen) by the addition of 0.2mM IPTG at 14^{o}C for 20 hours. After protein

expression, cells were collected and suspended in lysis buffer (50mM Tris pH 7.5, 150mM NaCl, 0.05% NP-40, 1mM PMSF, protease inhibitors, and 0.5mg/mL of lysozyme solution). The cells were incubated for 45 minutes at 4^{o}C and lysed using an EpiShear Probe Sonicator (Active Motif). Lysed cells were centrifuged and the supernatant was removed and incubated with Glutathione Sepharose 4B (GE). Recombinant GST fusion proteins were eluted by the addition of 15mg/mL of L-Glutathione (Sigma) dissolved in 100mM Tris pH 8.0. Recombinant proteins were resolved on a 4-12% Bis Tris gel and analyzed with Colloidal staining.

Calf Thymus Histone Binding Assays

Calf thymus histone binding assays were preformed by incubating 50μg of calf thymus histones (Worthington) with 10μg of recombinant GST fusion proteins in buffer (50mM Tris pH 7.5, 1M NaCl, and 1% NP-40) overnight. GST fusion protein histone interactions were assessed by adding Glutathione Sepharose 4B (GE) beads for 1 hour, washing 5 times in buffer then resuspended in 5xSDS sample buffer and run on a 4-12% Tris-Bis polyacrylamide gel, which was then transferred to a nitrocellulose membrane followed by western blot analysis.

MLA Histone Binding Assays

Similar to the calf thymus histone binding assay, 2μg of recombinant GST fusion proteins were incubated with 1μg of full length recombinant histone H3 with either no methylation on K4 or Methylated Lysine Analogs (K4me1, K4me2, and K4me3) (Active

Motif) in buffer (50mM Tris pH 7.5, 1M NaCl, and 1%NP-40) overnight. Glutathione Sepharose 4B (GE) beads were added for 1 hour, washed five times with buffer and the beads were resuspended in 5xSDS sample buffer. Proteins were resolved on a gel and interactions were assessed by transferring the proteins to a nitrocellulose membrane and using western blot analysis.

Chromatin Immunoprecipitation (ChIP)

Cells were grown to A_{600} O.D. of 1. Formaldehyde was added to a final concentration of 1%. Glycine was added to a final concentration of 125mM. Cell pellets were washed, collected, and resuspended in buffer (1M sorbitol, 50mM Tris-Cl pH 7.4, 10mM β-ME, and Zymolase®). Spheroplasts were collected and resuspended in buffer (50mM Tris-HCl, 5mM $CaCl_2$, pH 7.9) and incubated with micrococcal nuclease to digest the chromatin. The reaction was stopped by the addition of EDTA to a final concentration of 10mM. Soluble, digested chromatin was isolated by the addition of immunoprecipitation buffer (50mM HEPES/KOH, 140mM NaCl, 1mM EDTA, 1% Triton X-100, 0.1% Na-deoxycholate) and isolated by centrifugation. The supernatant containing the soluble chromatin was removed and proteins were immunoprecipitated by standard methods. The immuno-conjugated beads were washed in these buffers (50mM HEPES/KOH, 140mM NaCl, 1mM EDTA, 1% Triton X-100, 0.1% Na-deoxycholate), (50mM HEPES/KOH, 500mM NaCl, 1mM EDTA, 1% Triton X-100, 0.1% Na-deoxycholate), (10mM Tris-HCl, 0.25 M LiCL, 0.5% NP-40, 0.5% Na-deoxycholate, 1mM EDTA), and (50mM Tris-HCl, 10mM EDTA). The immunoprecipitate was eluted with (50mM Tris-

HCl, 10mM EDTA, 1% SDS), reverse crosslinked, treated with proteinase K, and the DNA was isolated using standard precipitation methods.

Nocodazole arrest and release

Cells were diluted into YPD media from overnight cultures and allowed to grow until a density of 10^7 cells per mL. Nocodazole was added to a final concentration of 15μg/mL and the cells were allowed to arrest for 2 hours. Cells were released from the G2/M arrest by washing twice in dH_2O, resuspended into fresh YPD media, and collected at the indicated time points.

Whole cell protein extracts preparation

An equal number of logarithmically growing yeast cells were collected, pelleted and the supernatant removed. Cells were then resuspended in 0.3M NaOH and 1.2% Beta mercaptoethanol) to lyse the cells and incubated for 10 minutes at 4^0 C. TCA was added to the mixture to a final concentration of 7% to precipitate the proteins and incubated for 10 minutes at 4^0 C. The precipitated proteins were then collected by centrifuging at 6000 rpm for 2 minutes at 4^0 C. The supernatant was removed and the pellet was washed with 1M unbuffered Tris. The protein pellet was centrifudged for 30 seconds at 14000 rpm and the supernatant removed. Whole cell extracts were resuspended in 5xSDS Sample Buffer and boiled for 5 minutes at 95^0 C.

Western Blot Analysis

Whole cell extracts were resuspended in of 5×SDS loading buffer and heated at 95°C for 5 minutes. Whole cell extracts were separated on a 4–12% polyacrylamide gel, transferred to a nitrocellulose membrane, blocked, blotted with the indicated antibodies (see Table 4), washed, and in incubated with the corresponding secondary antibodies (Sigma A0168, A0545; 1:10,000). Lastly membranes were visualized with ECL reagent.

Table 1: Yeast strains generated for this study

Strain	Genotype
yAS1	*MATa his3Δ1 leu2Δ0 met15Δ0 ura3Δ0*
yAS14	*MATa his3Δ1 leu2Δ0 met15Δ0 ura3Δ0 set1Δ:: kan^r*
yAS15	*MATa his3Δ1 leu2Δ0 met15Δ0 ura3Δ0 set2Δ::kan^r*
yAS21	*MATa his3Δ1 leu2Δ0 met15Δ0 ura3Δ0 set3Δ::kan^r*
yAS17	*MATa his3Δ1 leu2Δ0 met15Δ0 ura3Δ0 set4Δ::kan^r*
yAS25	*MATa his3Δ1 leu2Δ0 met15Δ0 ura3Δ0 set5Δ::kan^r*
yAS26	*MATa his3Δ1 leu2Δ0 met15Δ0 ura3Δ0 set6Δ::kan^r*
yAS19	*MATa his3Δ1 leu2Δ0 met15Δ0 ura3Δ0 set7Δ::kan^r*
yAS203	*MATa his3Δ1 leu2Δ0 met15Δ0 ura3Δ0 bre1Δ::kan^r*
yAS28	*MATa his3Δ1 leu2Δ0 met15Δ0 ura3Δ0 set1G951S*
yAS225	*MATa his3Δ1 leu2Δ0 met15Δ0 ura3Δ0 bre2-TAP::HIS*
yAS226	*MATa his3Δ1 leu2Δ0 met15Δ0 ura3Δ0 bre2-TAP::HIS set1Δ::KANMX*
yAS227	*MATa his3Δ1 leu2Δ0 met15Δ0 ura3Δ0 bre2-TAP::HIS set1G951S*
yAS93	*MATa his3Δ1 leu2Δ0 met15Δ0 ura3Δ0 swd1Δ::kan^r*
yAS75	*MATa his3Δ1 leu2Δ0 met15Δ0 ura3Δ0 swd3Δ::kan^r*
yAS90	*MATa his3Δ1 leu2Δ0 met15Δ0 ura3Δ0 sdc1Δ::kan^r*
yAS10	*MATa his3Δ1 leu2Δ0 met15Δ0 ura3Δ0 bre2Δ::kan^r*
yAS12	*MATa his3Δ1 leu2Δ0 met15Δ0 ura3Δ0 spp1Δ::kan^r*
yAS92	*MATa his3Δ1 leu2Δ0 met15Δ0 ura3Δ0 shg1Δ::kan^r*
yAS42	*MATa his3Δ1 leu2Δ0 met15Δ0 ura3Δ0 bub1Δ::kan^r*
yAS44	*MATa his3Δ1 leu2Δ0 met15Δ0 ura3Δ0 bub3Δ::kan^r*
yAS30	*MATa his3Δ1 leu2Δ0 met15Δ0 ura3Δ0 set1G951S bub1Δ::kan^r*
yAS32	*MATa his3Δ1 leu2Δ0 met15Δ0 ura3Δ0 set1G951S bub3Δ::kan^r*
yAS45	*MATa his3Δ1 leu2Δ0 met15Δ0 ura3Δ0 mad1Δ::kan^r*
yAS46	*MATa his3Δ1 leu2Δ0 met15Δ0 ura3Δ0 mad2Δ::kan^r*
yAS47	*MATa his3Δ1 leu2Δ0 met15Δ0 ura3Δ0 mad3Δ::kan^r*
yAS33	*MATa his3Δ1 leu2Δ0 met15Δ0 ura3Δ0 set1G951S mad1Δ::kan^r*
yAS34	*MATa his3Δ1 leu2Δ0 met15Δ0 ura3Δ0 set1G951S mad2Δ::kan^r*
yAS35	*MATa his3Δ1 leu2Δ0 met15Δ0 ura3Δ0 set1G951S mad3Δ::kan^r*
yAS129	*MATa his3Δ1 leu2Δ0 met15Δ0 ura3Δ0 dam1K233R*
yAS153	*MATa his3Δ1 leu2Δ0 met15Δ0 ura3Δ0 hht1K4R hht2K4R*
yAS36	*MATa his3Δ1 leu2Δ0 met15Δ0 ura3Δ0 hht1K4R hht2K4R bub1Δ::kan^r*
yAS38	*MATa his3Δ1 leu2Δ0 met15Δ0 ura3Δ0 hht1K4R hht2K4R bub3Δ::kan^r*
yAS39	*MATa his3Δ1 leu2Δ0 met15Δ0 ura3Δ0 hht1K4R hht2K4R mad1Δ::kan^r*

yAS40	*MAT*a *his3Δ1 leu2Δ0 met15Δ0 ura3Δ0 hht1K4R hht2K4R mad2Δ::kan^r*
yAS41	*MAT*a *his3Δ1 leu2Δ0 met15Δ0 ura3Δ0 hht1K4R hht2K4R mad3Δ::kan^r*
yAS229	*MAT*a *his3Δ1 leu2Δ0 met15Δ0 ura3Δ0 bre2-TAP::HIS hht1K4R hht2K4R*
yAS228	*MAT*a *his3Δ1 leu2Δ0 met15Δ0 ura3Δ0 bre2-TAP::HIS hht1K4R hht2K4R set1Δ::KANMX*
yAS232	*MAT*a *his3Δ1 leu2Δ0 met15Δ0 ura3Δ0 cdc20-127*
yAS233	*MAT*a *his3Δ1 leu2Δ0 met15Δ0 ura3Δ0 cdc20-127 set1G951S*
yAS237	*MATa his3Δ1 leu2Δ0 met15Δ0 ura3Δ0 cdc20-127 hht1K4R hht2K4R*
yAS234	*MATa his3Δ1 leu2Δ0 met15Δ0 ura3Δ0 PDS1-18MYC*
yAS235	*MATa his3Δ1 leu2Δ0 met15Δ0 ura3Δ0 PDS1-18MYC set1G951S*

Table 2: Primers used in this study for generation of deletion strains

Cassette:	Primer Name	Primer Sequence:
set1Δ::kan^r	SET1-550F-AS SET1-550R-AS	TGTTCAGTGAAGTATTATATAAA CACGAACATATTGTAATGATGGT
bre2Δ::kan^r	BRE2-500F-AS BRE2-500R-AS	CAGCCAATCTATCTTCCAGA CTATTTCTCCAGATAACTACA
spp1Δ::kan^r	SPP1-500F-AS SPP1-500R-AS	GAAACATTGCCTGCAGTCTC TTTATTACATGAGCTATCGTT
set2Δ::kan^r	SET2-500F-AS SET2-500R-AS	AGAAGAACAATCTATCATAA GGCGCGGCTAGATGTTTTGTT
set3Δ::kan^r	SET3-500F-AS SET3-500R-As	GGCCTTGCGGGCCTGCTGGC GATCCTAATGATGATGGCCAGT
set4Δ::kan^r	SET4-500F-AS SET4-500R-AS	TCTTCGCTTATACCCGTCTC TGCAAATGAGTTATAAGTTGAAG
set5Δ::kan^r	SET5-500F-AS SET5-500R-AS	GGTTTGCGAGCCTTACTATT ACAAGGTCAACAAGAACAGCA
set6Δ::kan^r	SET6-500F-AS SET6-500R-AS	AACTACACTTCGGTTGATAA CAATGGTATCAAATTTGAATT
set7Δ::kan^r	SET7-500F-AS SET7-500R-AS	TGAATAGATTAATTCATAGA ATATTTTCCCTGTTGAAATGAG
bub1Δ::kan^r	BUB1-500F-AS BUB1-500R-AS	AAAACATTCTCCTTTTGAGG GCTCAATATGAAAAAATGAA
bub3Δ::kan^r	BUB3-500F-AS BUB3-500R-AS	AAGAAGTTAAGACAGTTAAA AAGTGGGCGGCACCGAGTCT
mad1Δ::kan^r	MAD1-500F-AS MAD1-500R-AS	GTTTGGGCCACAATCTATAG GTAACCATCCCCATCCACCT
mad2Δ::kan^r	MAD2-500F-AS MAD2-500R-AS	AATAGCATTAAATTCCGGAT TGGTCTTTTGTCCTCGCTTT
mad3Δ::kan^r	MAD3-500F-AS MAD3-500R-AS	ACCAAAAGTTTACTTTGCCA ATTTTACAACAGGTATTGAT

Table 2: Primers used in this study for genotyping deletion strains

Cassette:	Primer Name	Primer Sequence:
set1Δ::kan^r	KAN-F-AS SET1-600R-AS	CCTCGACATCATCTGCCC TGACCCCATTTGTGTTAAAA
bre2Δ::kan^r	KAN-F-AS BRE2-550R-AS	CCTCGACATCATCTGCCC GTCGAATAACAAAGAAGGTATAG
spp1Δ::kan^r	KAN-F-AS SPP1-550R-AS	CCTCGACATCATCTGCCC ATTTCACTCCCTTGAGAATATAA
set2Δ::kan^r	KAN-F-AS SET2-550R-AS	CCTCGACATCATCTGCCC TGCATTGGCAACAGTATTTTTTC
set3Δ::kan^r	KAN-F-AS SET3-550R-AS	CCTCGACATCATCTGCCC TTCACCATCAGTTTGACTTTGAA
set4Δ::kan^r	KAN-F-AS SET4-550R-AS	CCTCGACATCATCTGCCC GTCACGAAGCTGTTGCCAAATTT
set5Δ::kan^r	KAN-F-AS SET5-550R-AS	CCTCGACATCATCTGCCC ACTACCCCTGTTACCCCAGGTGC
set6Δ::kan^r	KAN-F-AS SET6-550R-AS	CCTCGACATCATCTGCCC GGATCCTCCCAAATTTGAGTGGA
set7Δ::kan^r	KAN-F-AS SET7-500R-AS	CCTCGACATCATCTGCCC CAAAATAGCCGAAGGCACCAGAA
bub1Δ::kan^r	KAN-F-AS BUB1-550R-AS	CCTCGACATCATCTGCCC TTGTCGTTATTAGAGTAGGT
bub3Δ::kan^r	KAN-F-AS BUB3-550R-AS	CCTCGACATCATCTGCCC CCAAGGCTTTTTTGTAGTTG
mad1Δ::kan^r	KAN-F-AS MAD1-550R-AS	CCTCGACATCATCTGCCC AACAAGCTTTTCTGCCGTAG
mad2Δ::kan^r	KAN-F-AS MAD2-550R-AS	CCTCGACATCATCTGCCC ATTACGAGACCTACTCCAAA
mad3Δ::kan^r	KAN-F-AS MAD3-550R-AS	CCTCGACATCATCTGCCC TGATCCTATTAGACTCCTAT

Table 3: Plasmids generated for this study

Construct	Content	Content (Amino Acids) Mutations	Source:
pGEX4T1	GST	GST	GE Healthcare
pAS47	GST-Bub3-full length	GST-Bub3 (1-342)	This study
pAS28	GST-Cdc20-full length	GST-Cdc20 (1-611)	This study
pAS48	GST-Mad2-full length	GST-Mad2 (1-197)	This study
pAS119	GST-Mad2-Open	GST-Mad2 (1-191)	This study
pAS120	GST-Mad2-Closed	GST-Mad2 (1-197) R126E/Q127A	This study
pAS126	GST-Cdc20-Wd40	GST-Cdc20 (289-611)	This study
pAS128	GST-Cdc20-Wd40-G544R	GST-Cdc20 (289-611) G544R	This study

Chapter 3: Results

Loss of *SET1* induces benomyl resistance.

Our previous studies demonstrated that Set1 has unique functions in mitosis that are independent of its functions in transcriptional regulation (Zhang 2005; Latham, 2011). To further address how lysine methylation might regulate mitosis, we subjected cells bearing deletions in *SET1* or in other SET domain encoding genes, to growth in the presence of the microtubule depolymerizing agent, benomyl. Microtubule depolymerizing drugs interfere with mitotic spindle stability, blocking mitotic progression. Mutations in genes required for formation of the mitotic spindle, in components of the kinetochore, or in the activation and maintenance of mitotic checkpoints are characteristically sensitive to microtubule depolymerizing drugs.

Using a five-fold serial dilution assay coupled with increasing amounts of benomyl, we discovered that *set1* mutant cells are highly resistant, rather than sensitive, to high levels of benomyl. *SET1* cells grow similarly to wild type cells on rich media or in the presence of DMSO vehicle alone, but they display continued growth in levels of benomyl that completely block growth of wild-type cells. No other SET domain gene deletion resulted in a resistance phenotype, indicating a unique function for Set1 in responding to microtubule poisons (Figure 3). Interestingly, since *SET2* encodes the lysine methyltransferase required for histone H3 K36 mono-, di-, and tri-methylation, which is also associated with active transcription, our results suggest that defective transcription is not sufficient to induce benomyl resistance.

Figure 3: The *set1Δ* strain is resistant to benomyl

A serial five-fold dilution growth assay was used to reveal a resistance to benomyl phenotype. Strains were placed onto either control plates (YPD) or plates containing 30μg/mL of benomyl (BENOMYL). Plates were plated at 30^0 C for 2 days.

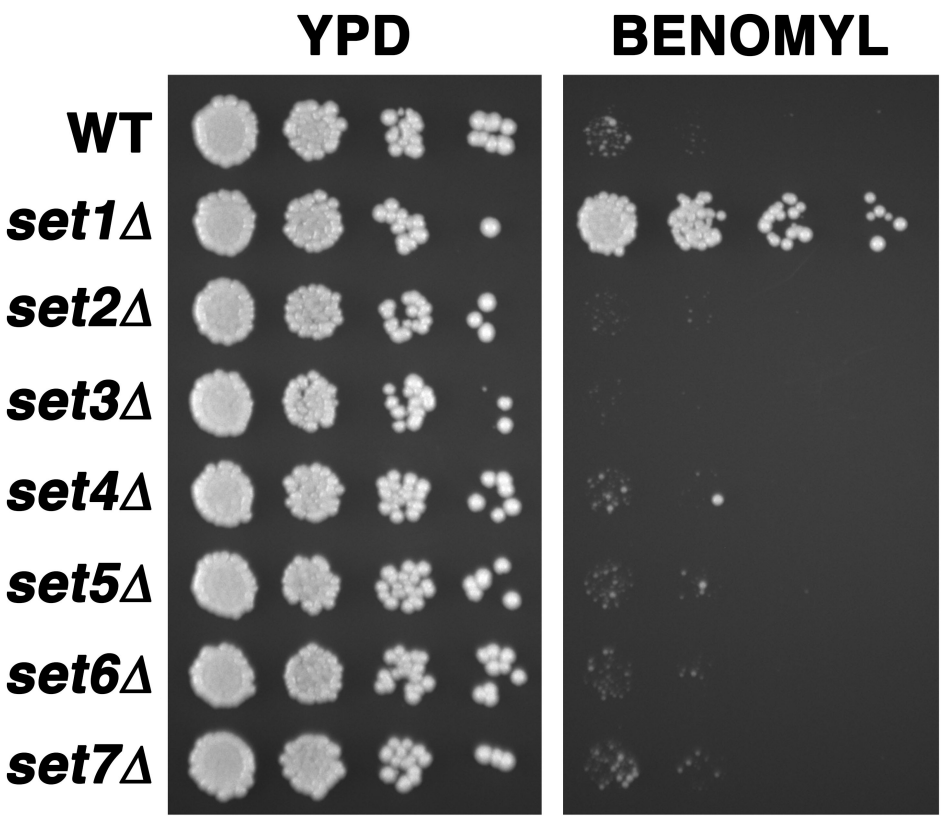

Figure 3

To address whether the benomyl resistance phenotype caused by *SET1* deletion reflects loss of Set1 catalytic activity, we subjected cells bearing a mutation in the Set1 catalytic site (Nagy et al., 2002) to growth in the presence of the drug. Importantly, although a recent report found that many mutations in Set that affect methyltransferase activity result in lower amounts of total Set1 protein (Soares et al., 2014), we detect equal amounts of wild-type Set1 and Set1G951S protein in whole cell extracts, as detected by immunoblot (Figure 4). Moreover, we find equal incorporation of wild type and mutant Set1 into the COMPASS complex, isolated via affinity purification of Bre2, another COMPASS component (Figure 5). As expected, the G951S mutation abrogated the ability of Set1 to methylate histone H3K4 (data not shown). Importantly, cells bearing the *set1G951S* mutation displayed benomyl resistance equivalent to that caused by *SET1* deletion (Figure 6), indicating Set1 catalytic activity is required for proper benomyl response.

These results are consistent with a large scale screen reported previously that indicated *BRE1* mutants display resistance to benomyl (Rieger et al., 1999). Bre1 is a targeting factor for the Rad6 ubiquitin ligase that is required for histone H2B K123 mono-ubiquitination (Nakanishi et al., 2009), an upstream event required for Set1 mediated methylation of both H3 K4 and Dam1 K233 (Latham et al., 2011; Lee et al., 2007a).

Figure 4: Total Set1 protein in wild-type and *set1* mutants

Whole cell extracts from WT (*SET1*), *set1Δ*, and the *set1G951S* strain were prepared and resolved on a gel. Pgk1 was used as a loading control.

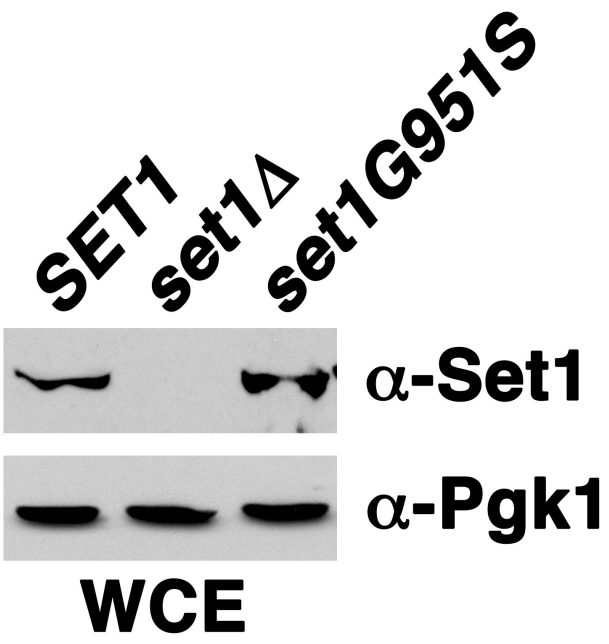

Figure 4

Figure 5: Incorporation of WT and Set1G951S proteins into COMPASS

Wild-type Set1 and Set1G951S proteins both similarly associate with the COMPASS component Bre2. Immunoprecipitation (IP) assays were used to pull down Bre2 and the associated levels of Set1 was assessed in wild-type (WT) and *set1G951S* strains. Bre2-TAP (α-Protein A) and Pgk1 (α-Pgk1) were used as loading controls.

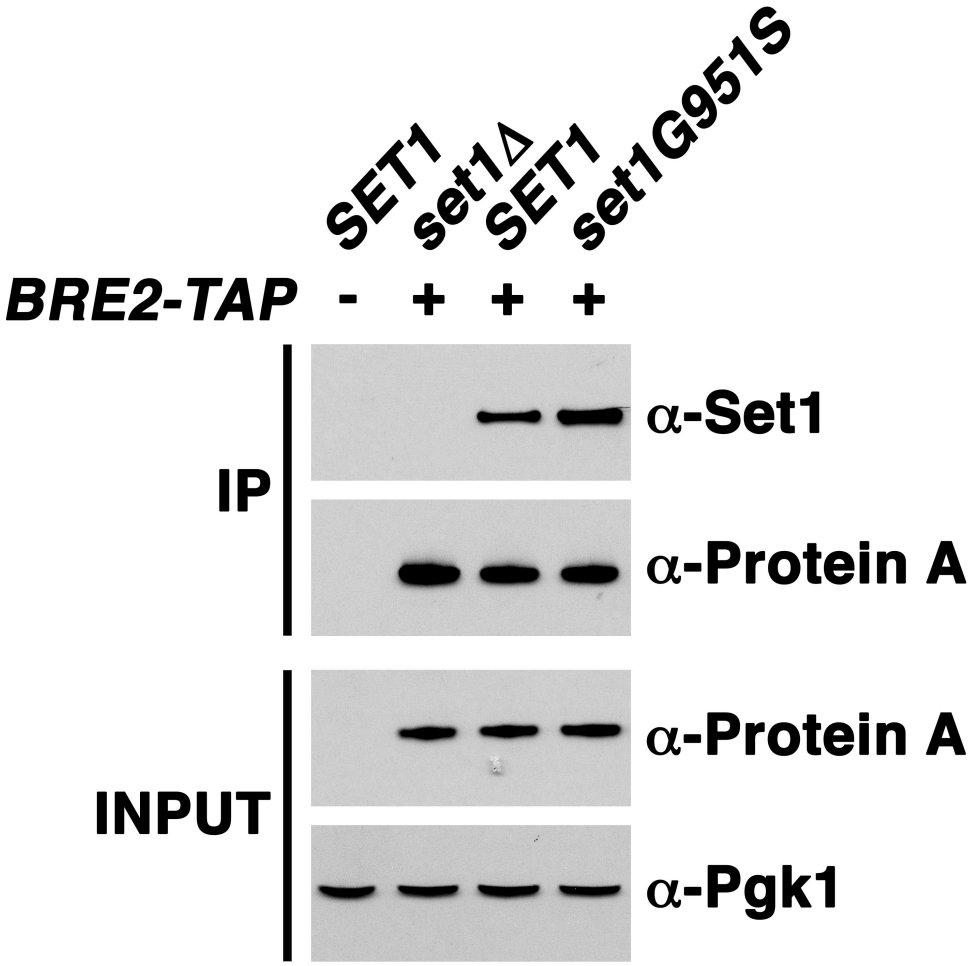
SET1
set1Δ
SET1
set1G951S
BRE2-TAP - + + +
IP
α-Set1
α-Protein A
INPUT
α-Protein A
α-Pgk1

Figure 5

Figure 6: The *bre1Δ, set1Δ*, and *set1G951S* strains are resistant to benomyl

A serial five-fold dilution growth assay of yeast strains with the indicated genotypes was performed to visualize growth phenotypes. Cells were placed onto YPD plates (YPD) or plates containing 30μg/mL of benomyl (BENOMYL) and incubated at 30^0C for 2 days.

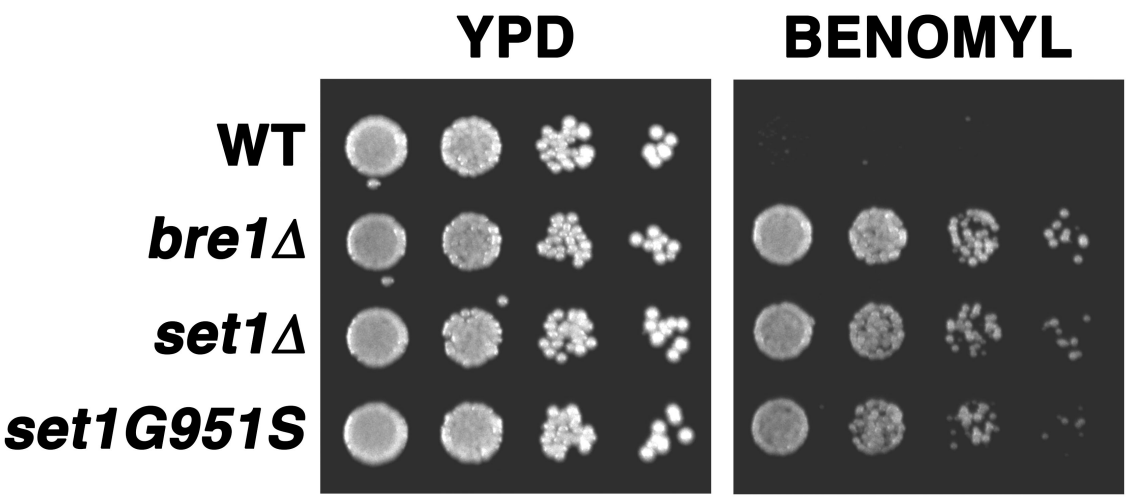

Figure 6

Different components of the COMPASS complex appear to contribute to mono-, di-, or tri-methylation of Set1 substrates. We find that deletion of genes encoding subunits required for all three methylation states, such as *SWD1* and *SWD*3, also results in benomyl resistance (Figure 7). Deletion of *BRE2* or *SDC1* reduces dimethylation and inhibits trimethylation of H3K4, and these mutations also induce substantial resistance to benomyl, although not quite to the same degree as caused by *SET1* mutations. Deletion of *SPP1* eliminates trimethylation of H3K4 without affecting mono- and dimethylation. Interestingly, *spp1* mutants display only a slight benomyl resistance, indicating that loss of trimethylation of COMPASS substrates is not sufficient to trigger resistance. Deletion of *SHG1* is reported to increase di- and trimethylation of H3K4. This deletion also fails to induce benomyl resistance. Together, these results indicate that mono- and dimethylation of substrates by Set1, working within the COMPASS complex, is required for proper response to microtubule poisons.

The benomyl resistance phenotype could be a downstream affect of additional cell cycle defects caused by *set1* mutations. Contrary to experiments previously described (Nislow et al., 1997), the *set1Δ* cells used here do not display any aberrations in cell cycle distribution as measured by flow cytometry (Figure 8) and a budding index assay (Figure 9). Consistent with previous data (Miller et al., 2001), our *set1Δ* cells do grow at a marginally slower rate compared to wild-type cells (Figure 10), and this slow growth correlates with a slightly reduced count in colony forming units (Figure 10). Lastly, no abnormal cellular morphology phenotypes were observed (Figure 11).

Figure 7: COMPASS mutants are benomyl resistant

A serial five-fold dilution growth assay of yeast strains with the indicated genotypes was performed to visualize growth phenotypes. Cells were placed onto YPD plates (YPD) or plates containing 30μg/mL of benomyl (BENOMYL) and incubated at 30^0 C for 2 day

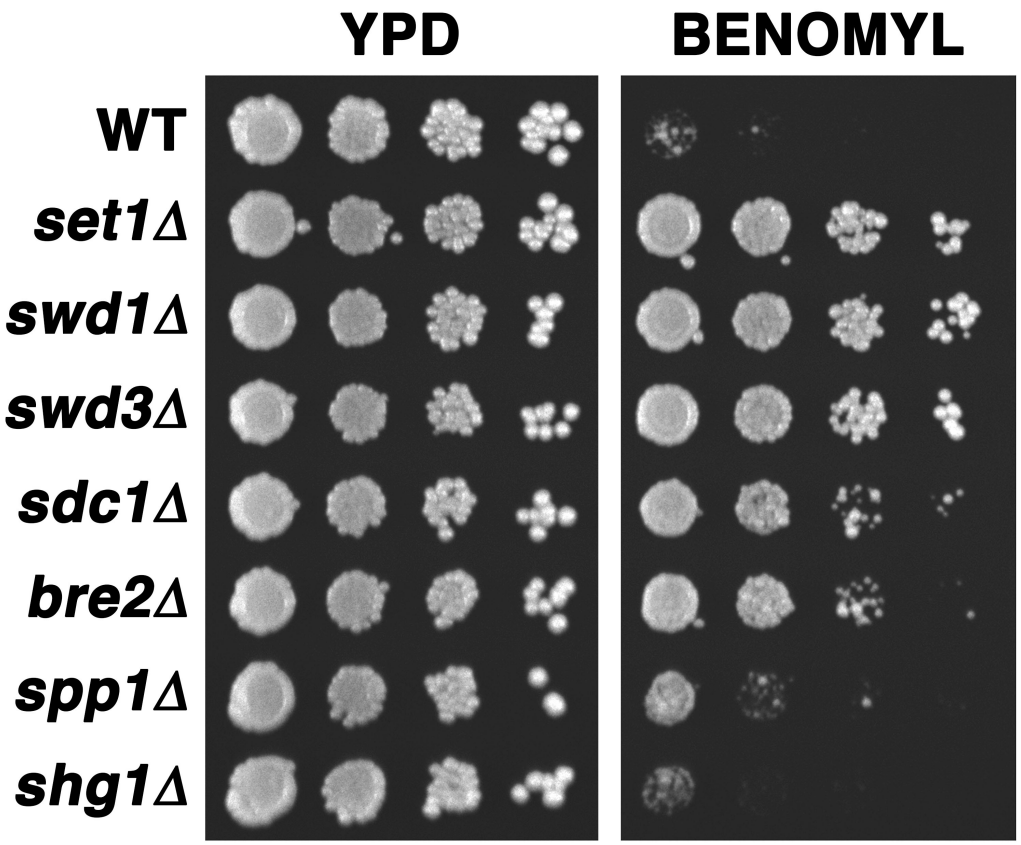

Figure 7

Figure 8: Cell cycle distribution of wild-type and *set1Δ* cells

Cell cycle analysis was assessed in both wild-type (blue) and *set1Δ* (red) asynchronous cultures. Cells were subjected to DNA labeling, flow cytometry analysis, and corresponding histograms were generated. Peaks associated with cells in G1 and G2 are labeled accordingly.

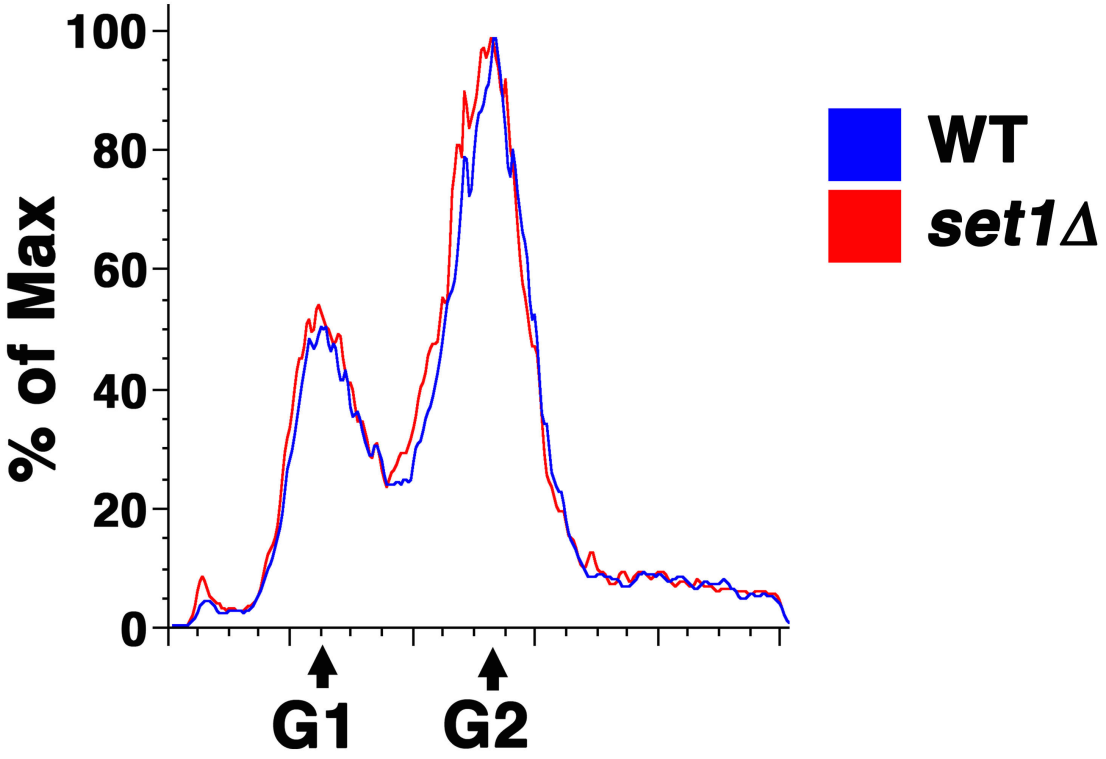

Figure 8

Figure 9: Budding index of wild-type and *set1Δ* cells

The budding index of wild-type (WT) and *set1Δ* cells was assessed by dividing fixed cells into three categories; cells with no bud, cells with a small bud, and cells with a large bud. These categories correspond to G1, S, and G2/M, respectively.

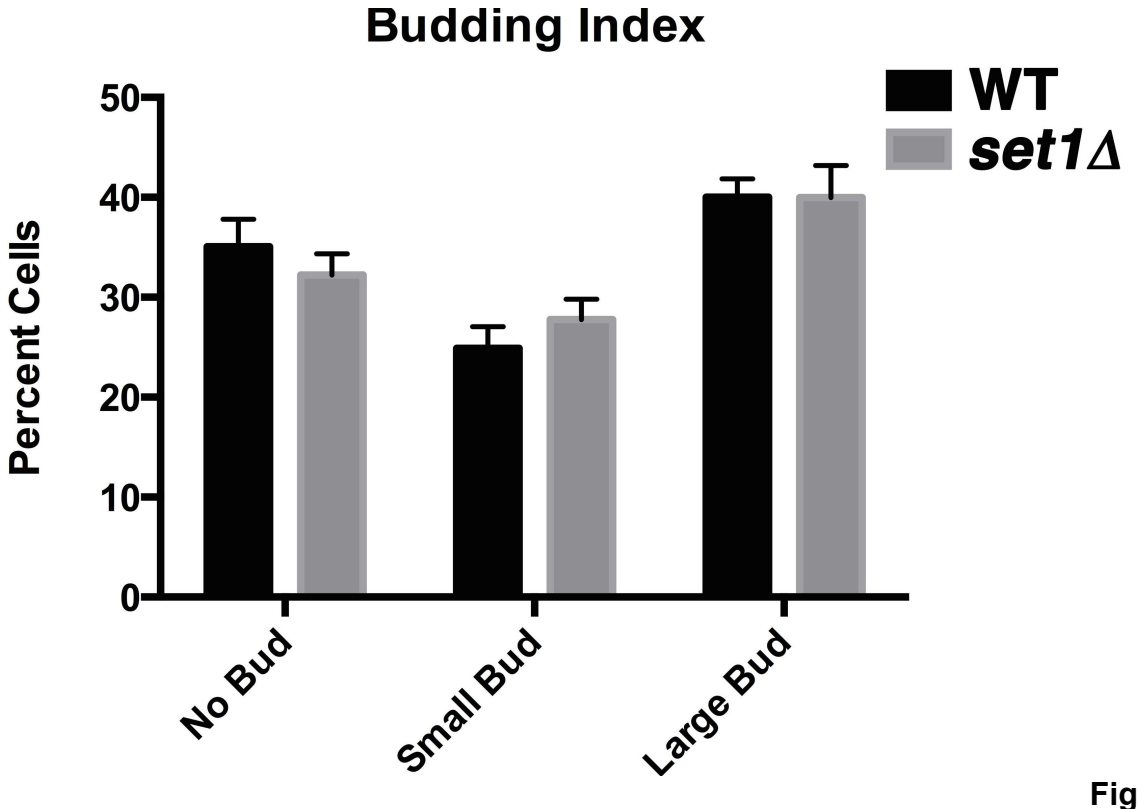
Budding Index
WT
set1Δ
Percent Cells
50
40
30
20
10
0
No Bud
Small Bud
Large Bud

Figure 9

Figure 10: Growth and colony forming assays of wild-type and *set1Δ* cells

Overnight cultures were diluted into fresh media and cell growth was assessed by Optic Density (O.D.) over time in both wild-type (WT) and *set1Δ* cells (top panel). In addition, equal amounts of wild-type (WT) and *set1Δ* cell cultures were taken from these growth assays at the indicated time points and assessed for cell viability by counting colongy forming units on normal YPD plates (bottom panel).

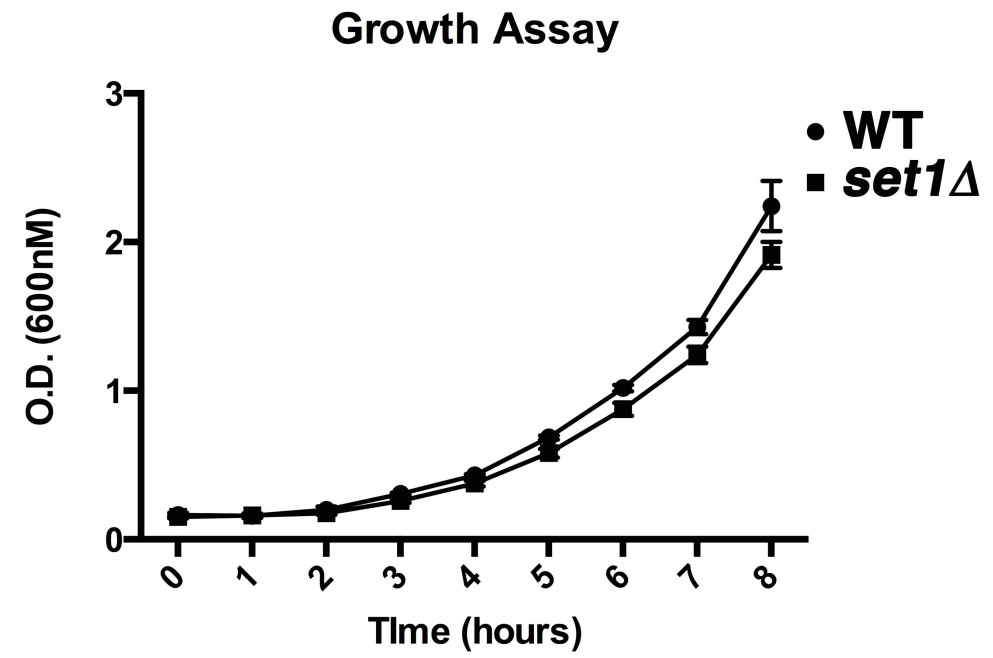
Growth Assay
O.D. (600nM)
3
2
1
0
0 1 2 3 4 5 6 7 8
Time (hours)
WT
set1Δ

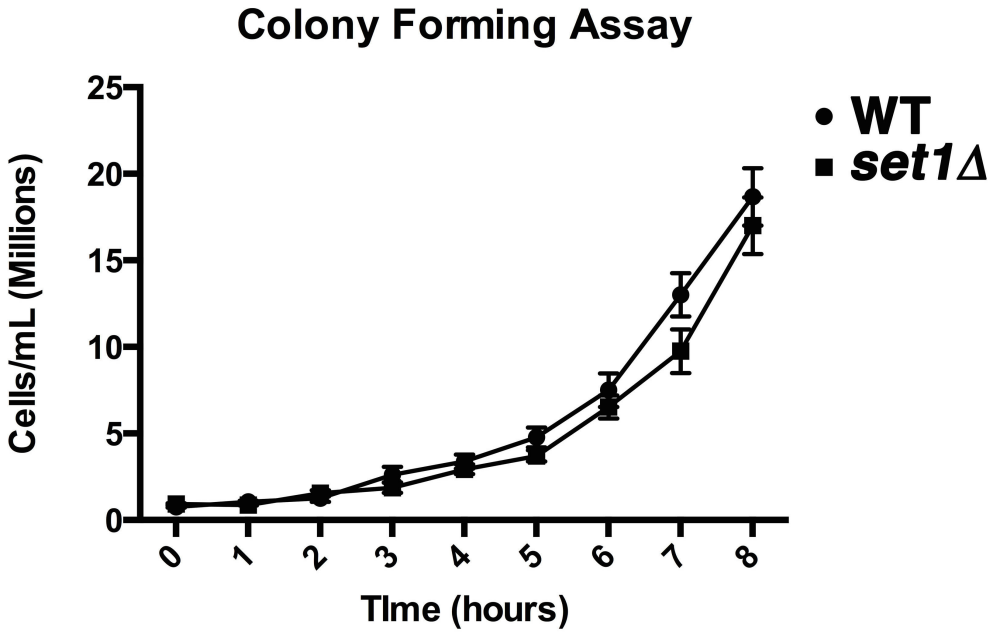
Colony Forming Assay
Cells/mL (Millions)
25
20
15
10
5
0
0 1 2 3 4 5 6 7 8
Time (hours)
WT
set1Δ

Figure 10

Figure 11: Wild-type and *set1Δ* cells display a similar cell morphology.

Yeast strains were fixed and Differential Interface Contrast (DIC) images were taken to assess overall cell shape, size, and morphology,

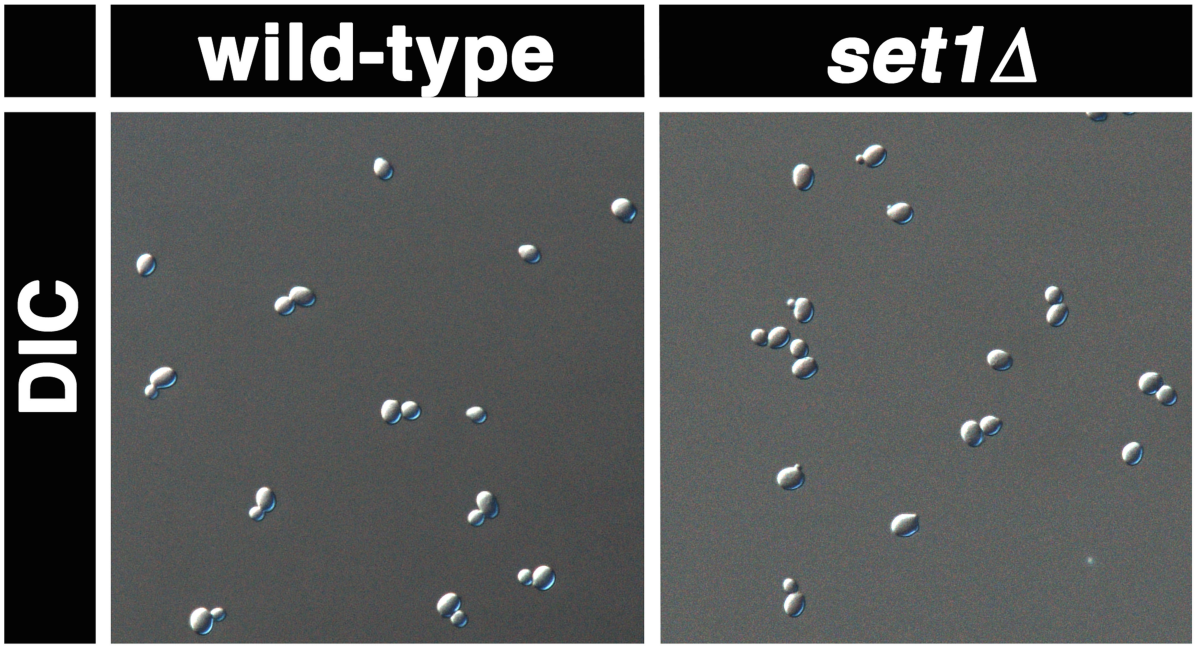

Figure 11

Therefore, the benomyl resistance phenotype displayed by *set1* mutants is unlikely to be a downstream affect of other cell cycle anomalies.

Benomyl resistance of *set1G951S* cells requires an intact Spindle Assembly Checkpoint and Cdc20 inhibition.

Resistance to benomyl and other spindle poisons could reflect a failure of cells to take up the drug or a failure in regulation of the Spindle Assembly Checkpoint among other possibilities. To determine if activation of the SAC is required for the benomyl resistance of *set1* mutants, we deleted genes encoding SAC components in the *set1G951S* strain. We found that deletion of *BUB1* and *BUB3* eliminated the resistance of *set1G951S* cells to benomyl (Figure 12). These data indicate that these SAC components are required for the resistance phenotype and also that the *set1* mutation does not prevent uptake of the drug, as the double mutants displayed a sensitivity to benomyl similar to that of *bub1* and *bub3* single mutants. Deletion of *MAD1*, *MAD2*, and *MAD3* also suppressed the benomyl resistance phenotype of *set1G951S* cells (Figure 13). Collectively, these data indicate that the SAC must be activated and intact for the benomyl resistance to occur in the *set1* mutant cells.

SAC component proteins bind to and inhibit Cdc20 to block entry into anaphase upon disruption of microtubule-kinetochore interactions. To further define the role of SAC activation in the benomyl resistance phenotype, we introduced a mutation that blocks CDC20 inhibition into *set1G951S* cells. The *cdc20-127* mutation is a dominant allele that blocks binding of Mad2 and Mad3 to Cdc20, thereby inhibiting SAC mediated cell

Figure 12: The SAC is required for the benomyl resistance of *set1* mutants

Serial five fold dilution assay of yeast strains with the indicated genotypes placed onto YPD plates (YPD) or YPD plates containing 30μg/mL of benomyl (BENOMYL). Cells were then incubated at 30^0 C for 2 days.

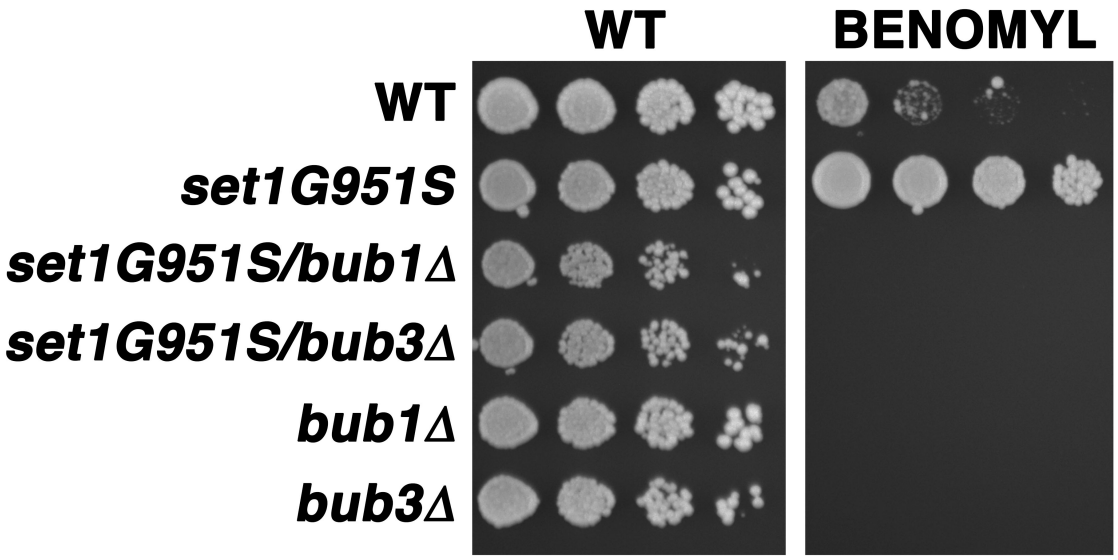
WT
BENOMYL
WT
set1G951S
set1G951S/bub1Δ
set1G951S/bub3Δ
bub1Δ
bub3Δ

Figure 12

Figure 13: The SAC is required for the benomyl resistance of *set1* mutants

Serial five fold dilution assay of yeast strains with the indicated genotypes placed onto YPD plates (YPD) or YPD plates containing 30μg/mL of benomyl (BENOMYL). Cells were then incubated at 30^0 C for 2 days.

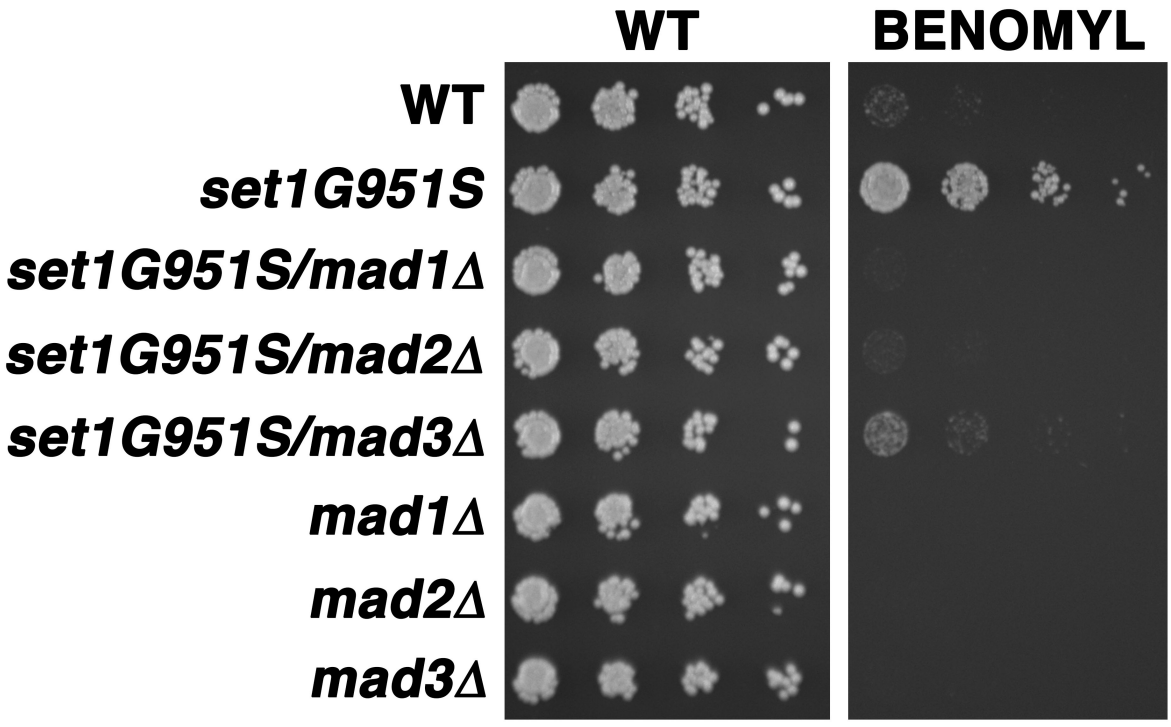
WT
BENOMYL
WT
set1G951S
set1G951S/mad1Δ
set1G951S/mad2Δ
set1G951S/mad3Δ
mad1Δ
mad2Δ
mad3Δ

Figure 13

cycle arrest (Hwang et al., 1998). We found that *set1G951S cdc20-127* double mutants are sensitive to benomyl compared to *set1G951S* mutants alone, indicating that binding of SAC components to Cdc20 is required for the benomyl resistance phenotype (Figure 14). Our data suggest loss of *SET1* mediated lysine methylation creates a benomyl resistance phenotype that requires Cdc20 inhibition and might reflect an overactive SAC in the presence of the *set1* mutant.

One phenotype reported previously for a temperature sensitive mutant of Cdc20, *cdc20-1*, has a thick mitotic spindle (Sethi et al., 1991), although this phenotype appears to be variable. We evaluated the mitotic spindle in our *set1* mutant cells using confocal microscopy, and we observed increase in fluorescence consistent with a thicker mitotic spindle in the *set1G951S* strain compared to wild-type cells (Figure 15). The mitotic spindle defect displayed by the *set1G951S* mutants suggests that loss of lysine methylation of a Set1 substrate may contribute to inhibition of Cdc20.

To further address SAC activation and release in *set1G951S* cells, we monitored Pds1 destruction by the APC. Pds1 (Securin) is a key substrate of the APC, and its ubiquitination and proteolysis are required for separation of sister chromatids and progression to anaphase. We treated both wild-type and *set1G951S* cells with nocodazole to activate the Spindle Assembly Checkpoint. Flow cytometry indicated that both wild-type and *set1G951S* cells arrested in G2/M, as expected. The cells were then released into fresh media, without drug, and mitotic progression was monitored by assessing Pds1 stability coupled with cell cycle analysis. Immunoblots indicate that

Figure 14: Cdc20 inhibition is required for the benomyl resistance of *set1* mutants

Serial five fold dilution growth assay of yeast strains with the indicated genotypes placed onto YPD plates (YPD) or YPD plates containing 30μg/mL of benomyl (BENOMYL). Cells were then incubated at 30^0 C for 2 days.

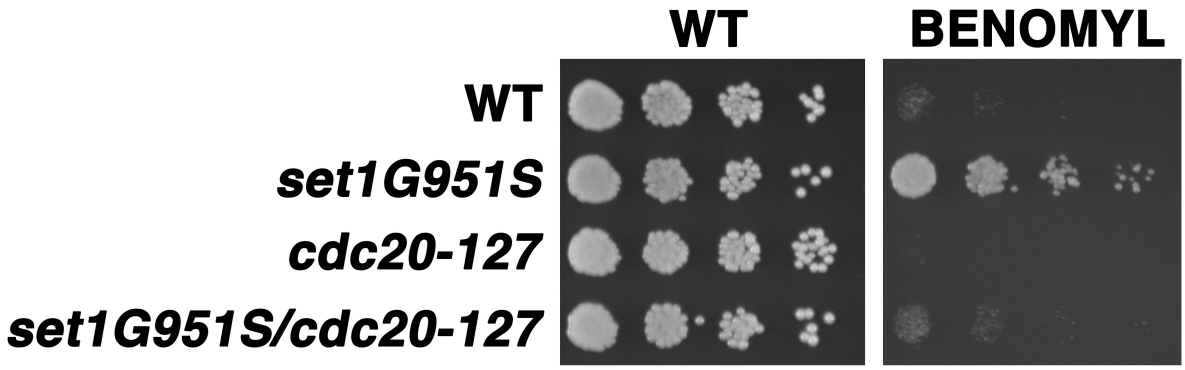

Figure 14

Figure 15: *set1G951S* mutants have a thicker mitotic spindle

SET1 catalytic mutant cells (set1G951S) display a more robust mitotic spindle staining compared to wild-type cells (WT). Immunofluorescence confocal images of wild-type and *set1G951S* mitotic cells are shown. Tubulin (green) and DAPI (blue) were used to identify cells undergoing mitosis from an asynchronous culture. Mitotic cells are outlined in white.

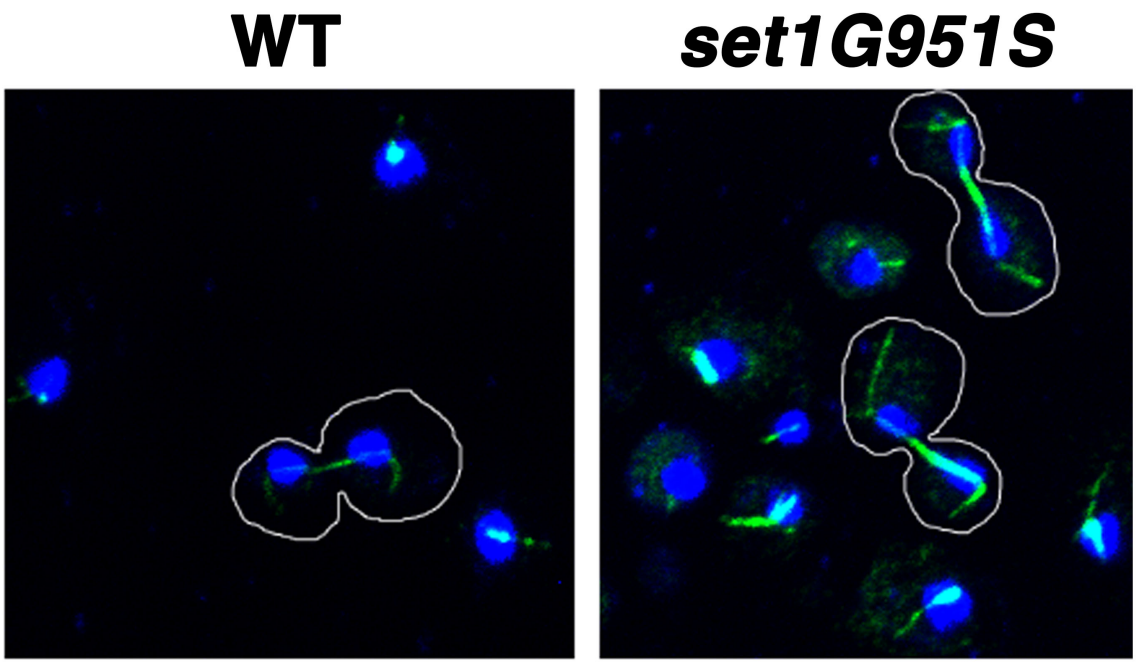

Figure 15

Pds1 is degraded at a slower rate in *set1* mutant cells, (Figure 16). These results indicate that *set1* mutants arrest normally after SAC activation, but they exhibit prolonged inhibition of the APC after checkpoint release.

Loss of histone H3 K4 methylation results in a benomyl resistance and mitotic spindle phenotype.

Two COMPASS substrates have been identified so far in yeast, histone H3K4 (Briggs et al., 2001) and Dam1 K233 (Zhang et al., 2005). We created yeast cells bearing mutations in these methylation sites in histone H3 and Dam1 in order to determine if either of these COMPASS substrates plays a role in regulating cellular responses to mitotic poisons. We found that *dam1K233R* bearing cells are sensitive to benomyl, much like wild-type cells. However, cells bearing mutations blocking histone H3K4 methylation (*H3K4R*) display benomyl resistance to a degree very similar to that of the *set1G951S* cells (Figure 17). Importantly, we confirmed that Set1 protein levels and incorporation into the COMPASS complex are not affected by the H3K4R mutation (Figure 18). Together these data indicate that H3K4 methylation by Set1 plays a role in cellular response to microtubule depolymerizing drugs.

To determine if histone H3K4 mutants also display a more robust staining of the mitotic spindle as seen in the *set1G951S* strain, we performed immunofluorescence staining of polymerized tubulin in wild-type, *dam1K233R*, *H3K4R*, and *set1G951S* yeast (Figure 19). The mitotic spindle in the *dam1K233R* strain appeared similar to that in wild-type cells. In contrast, the mitotic spindle in the *H3K4R* strain resembled that seen in the

Figure 16: Pds1 degrades more slowly in *set1* mutant cells

Cell cycle arrest and release experiments reveal that Pds1 is more stable in *set1* mutants (*set1G951S*) than in wild-type cells (WT). Cells were arrested in G2/M using nocodazole and released into fresh media. Samples were taken at the indicated time points, whole cell extracts and immunoblots were prepared and probed with α-Myc antibody to assess the protein levels of Myc-Pds1. Western blots for Pgk1 served as a loading control. Cells from the indicated time points were taken for analysis using flow cytometry. Histograms of DNA content reveal the cell cycle profile of the indicated strains at specific times after cell cycle arrest and release.

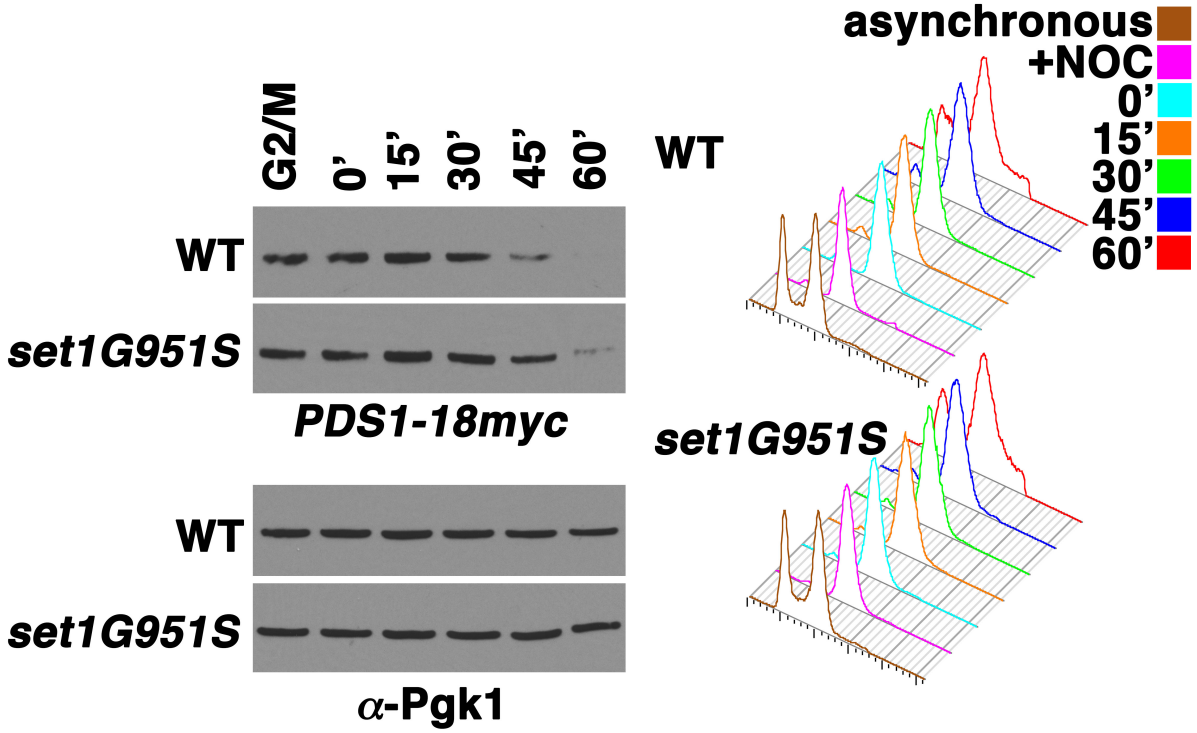
G2/M
0’
15’
30’
45’
60’
WT
set1G951S
PDS1-18myc
WT
set1G951S
α-Pgk1
WT
asynchronous
+NOC
0’
15’
30’
45’
60’
set1G951S

Figure 16

Figure 17: *H3K4R* mutants are benomyl resistant

Serial five fold dilution growth assay of wild-type (WT) and mutants with the indicated genotype placed onto either control plates (YPD) or plates containing 30μg/mL of benomyl (BENOMYL). Cells were incubated at 30^0C for 2 days.

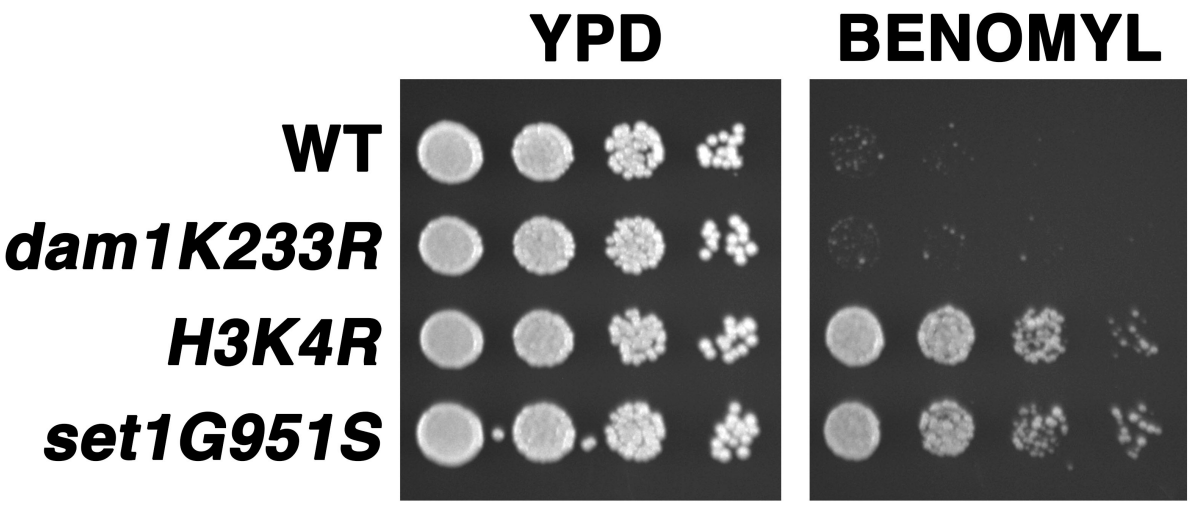

Figure 17

Figure 18: Incorporation of Set1 proteins into COMPASS in wild-type and mutant cells

Set1 proteins similarly associate with the COMPASS component Bre2 in *SET1, set1G951S,* and *H3K4R* mutant cells. Immunoprecipitation (IP) assays were used to pull down Bre2 and the associated levels of Set1 protein was assessed using α-Set1. Bre2-TAP (α-Protein A) and Pgk1 (α-Pgk1) were used as loading controls.

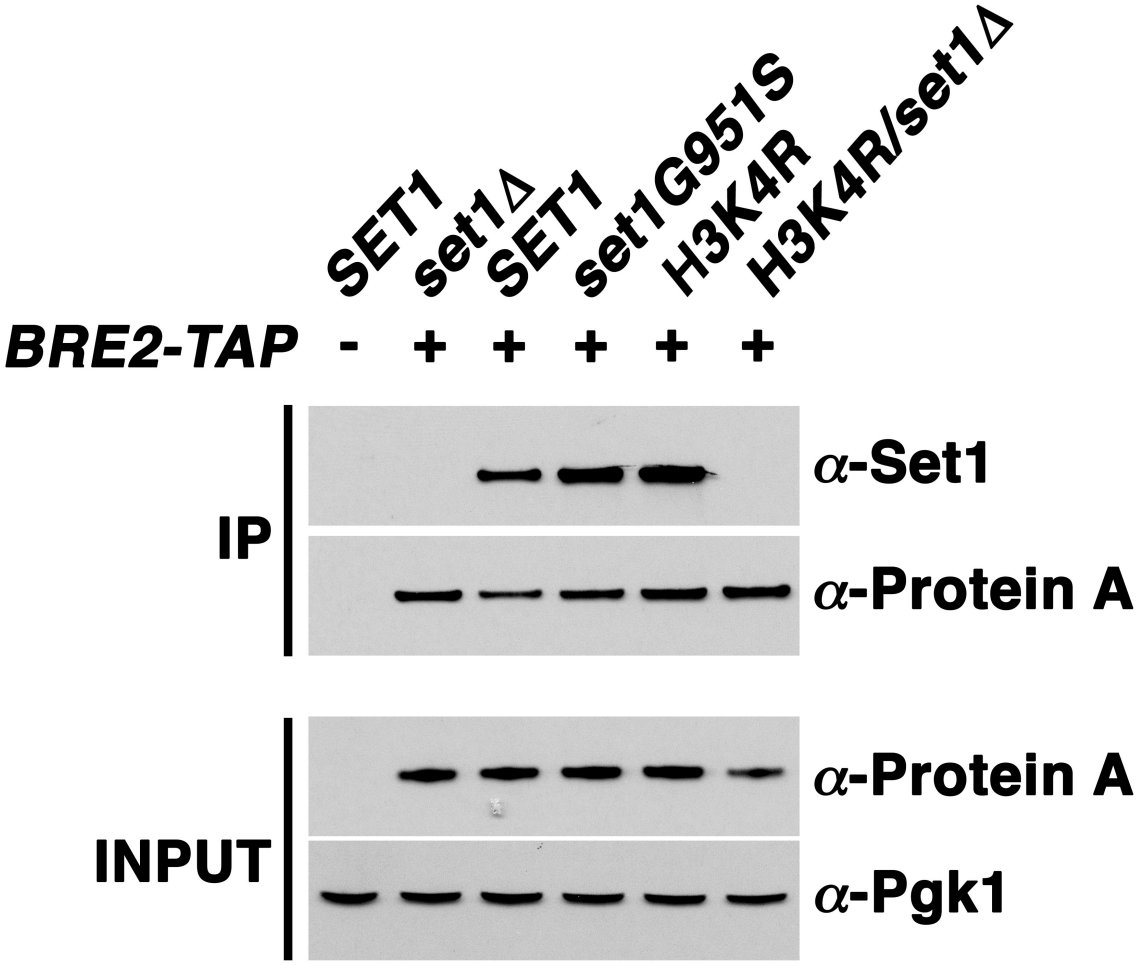
SET1
set1Δ
SET1
set1G951S
H3K4R
H3K4R/set1Δ
BRE2-TAP - + + + + +
IP
α-Set1
α-Protein A
INPUT
α-Protein A
α-Pgk1

Figure 18

Figure 19: *H3K4R* mutants have a thick mitotic spindle

Immunofluorescent images of wild-type (WT) and mutants with the indicated genotype. Images of mitotic cells were taken on a confocal microscope. Tubulin (green) and DAPI (blue) were used to identify cells undergoing mitosis from an asynchronous culture. Mitotic cells are outlined in white.

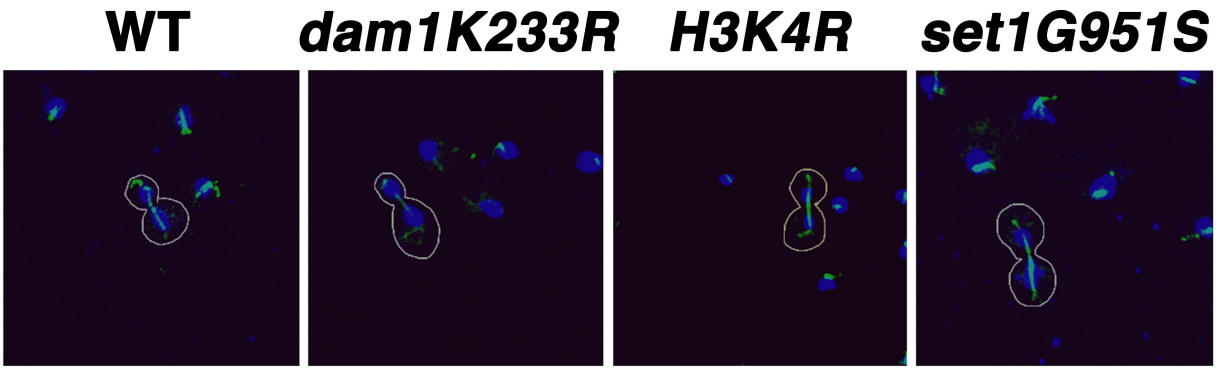

Figure 19

Figure 20: The SAC is required for the benomyl resistance of *H3K4R* mutants

Serial five fold dilution growth assay of wild-type (WT) and mutants with the indicated genotype placed onto either control plates (YPD) or plates containing 30μg/mL of benomyl (BENOMYL). Cells were incubated at 30^0 C for 2 days.

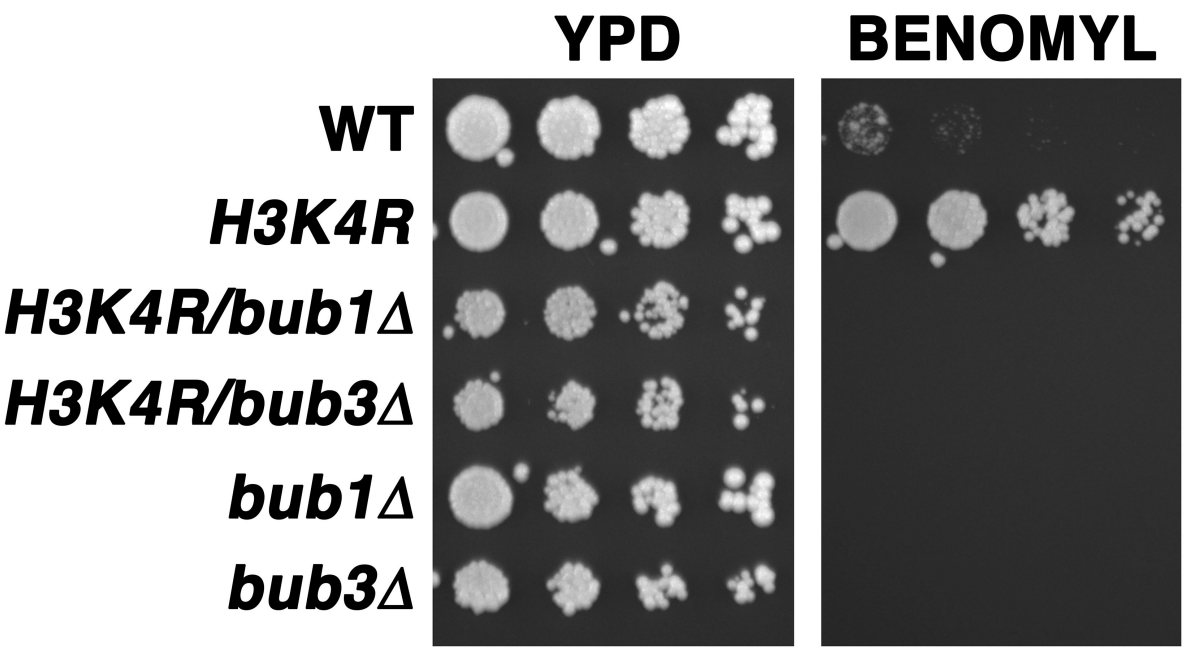

Figure 20

Figure 21: The SAC is required for the benomyl resistance of *H3K4R* mutants

Serial five fold dilution assay of wild-type (WT) and mutants with the indicated genotype placed onto either control plates (YPD) or plates containing 30μg/mL of benomyl (BENOMYL). Cells were incubated at 30^0 C for 2 days.

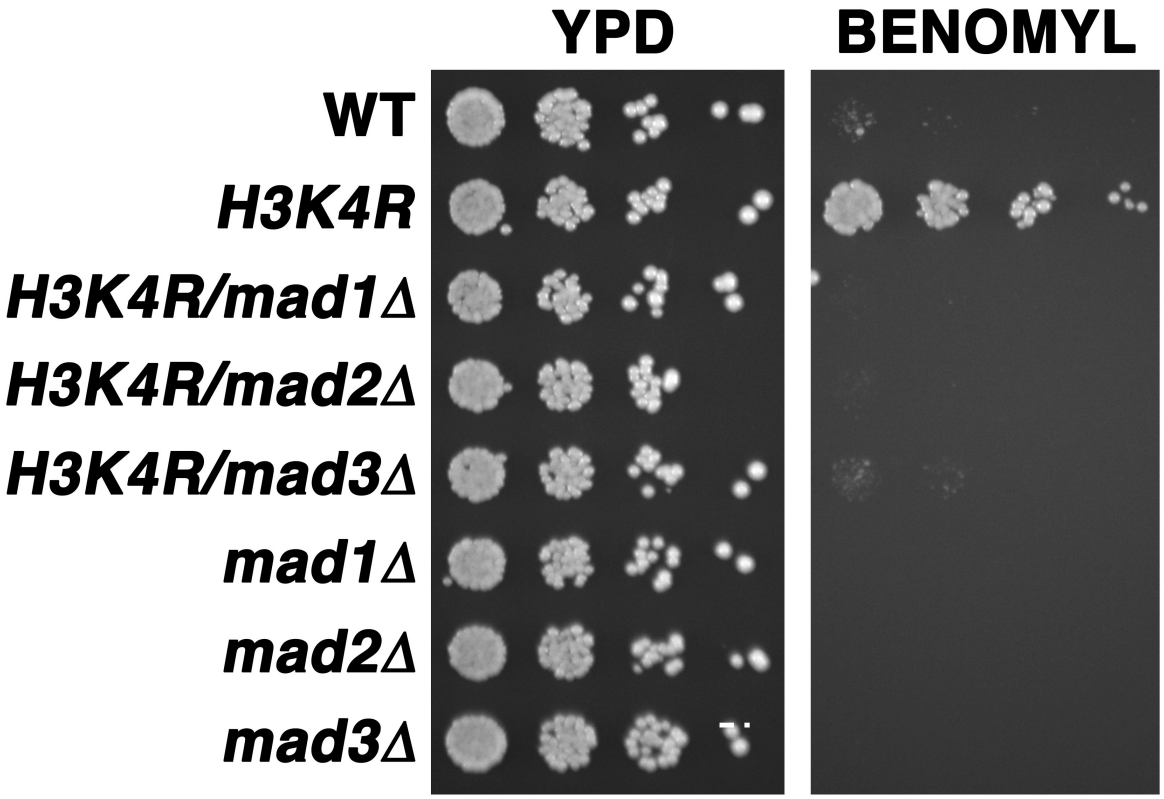
YPD
BENOMYL
WT
H3K4R
H3K4R/mad1Δ
H3K4R/mad2Δ
H3K4R/mad3Δ
mad1Δ
mad2Δ
mad3Δ

Figure 21

Figure 22: Loss of SAC components has no effect on H3K4 methylation

Whole cell extracts taken from wild-type (WT), *set1Δ*, and *mad2Δ* cells to compare di- and tri-methylation of histone H3 with immunoblots. Total H3 was used as a loading control.

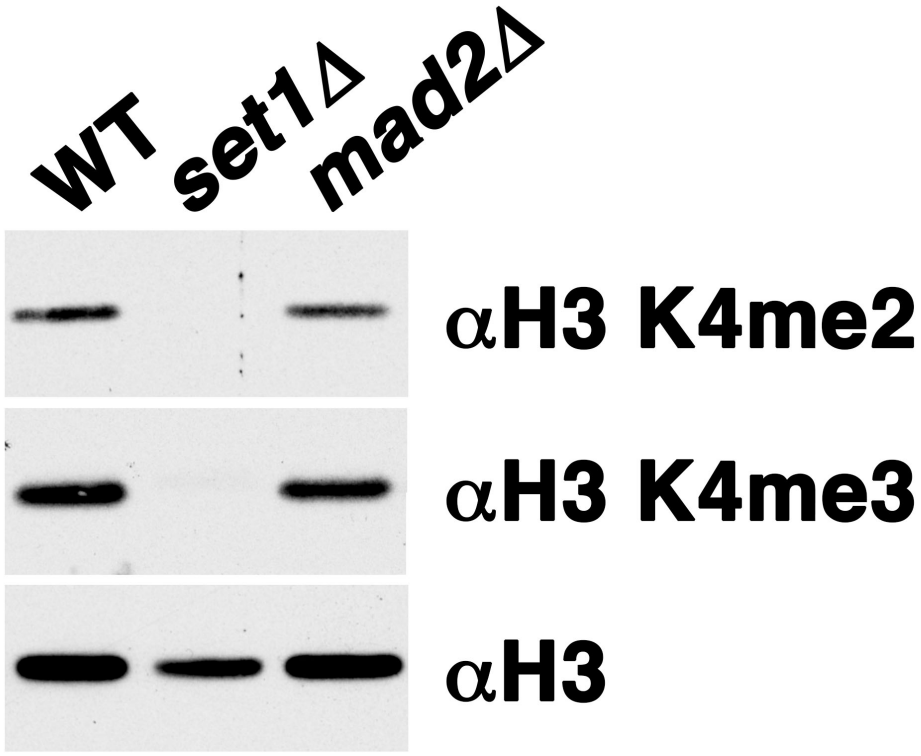

Figure 22

set1G951S cells, displaying a more robust staining of polymerized tubulin, or a “thick” mitotic spindle phenotype, relative to wild type cells. These data indicate that methylation of histone H3K4 plays a novel role in regulating the response to microtubule depolymerizing drugs, possibly related to increased amounts of polymerized tubulin or increased stability of the mitotic spindle.

To confirm that the benomyl resistance phenotype displayed by the *H3K4R* mutant requires an intact Spindle Assembly Checkpoint (SAC), as seen in *set1G951S* cells, we created yeast bearing both the histone *H3K4R* mutation and mutations in SAC components. Like the *set1G951S* strain, deletion of *SAC* component genes suppresses the benomyl resistance phenotype caused by the *H3K4R* mutation (Figure 20 and 21). Immunoblots confirm that loss of SAC components such as Mad2 has no effect on H3K4 methylation events, as H3K4 di- and trimethylation was unaltered in *mad2Δ* cells compared to wild-type cells (Figure 22). Immunofluorescence staining of the mitotic spindle in wild-type, *H3K4R*, *mad2Δ*, and *H3K4R/mad2Δ* cells indicates that eliminating SAC function through deletion of *MAD2* in *H3K4R* cells also results in loss of the thick mitotic spindle phenotype seen in *H3K4R* mutant cells (Figure 23). These data further link the mitotic spindle phenotype with the benomyl resistance observed in the *H3K4R* mutant cells, and indicate that loss of H3K4 methylation is affecting the SAC. To test whether the *H3K4R* mutant also regulates the SAC through Cdc20 inhibition, we introduced the *cdc20-127* mutation into the *H3K4R* strain. Like the *set1G951S* strain, the *H3K4R* strain requires Cdc20 inhibition for benomyl resistance (Figure 24) supporting the model of an overactive SAC when H3K4 methylation is inhibited.

Figure 23: The thick mitotic spindle of *H3K4R* mutants requires the SAC

Immunofluorescent images of wild-type (WT) and mutants with the indicated genotype. Images of mitotic cells were taken on a confocal microscope. Tubulin (green) and DAPI (blue) were used to identify cells undergoing mitosis from an asynchronous culture. Mitotic cells are outlined in white.

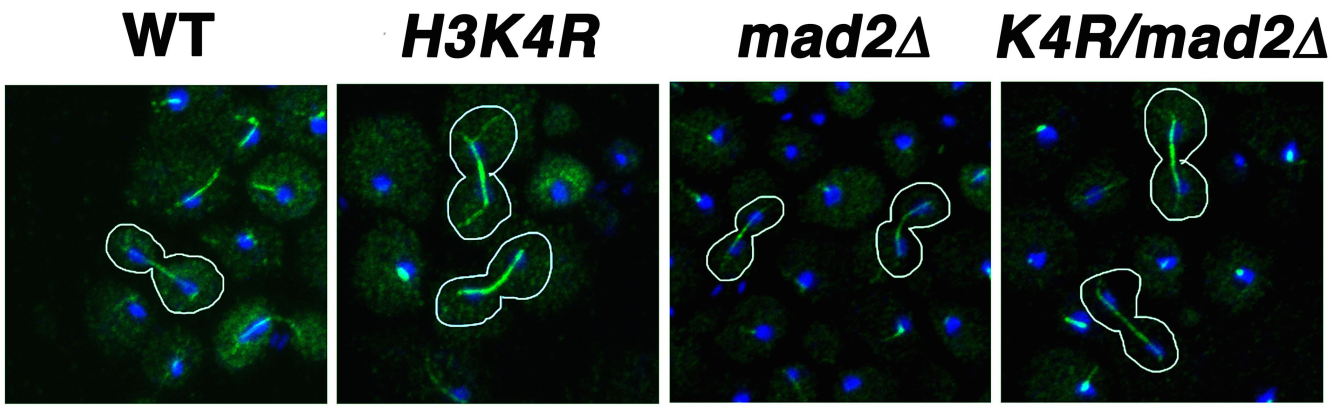

Figure 23

Figure 24: **Cdc20 inhibition is required for the benomyl resistance of *H3K4R* mutants**

Serial five fold dilution growth assay of wild-type (WT) and mutants with the indicated genotype placed onto either control plates (YPD) or plates containing 30μg/mL of benomyl (BENOMYL). Cells were incubated at 30^0 C for 2 days.

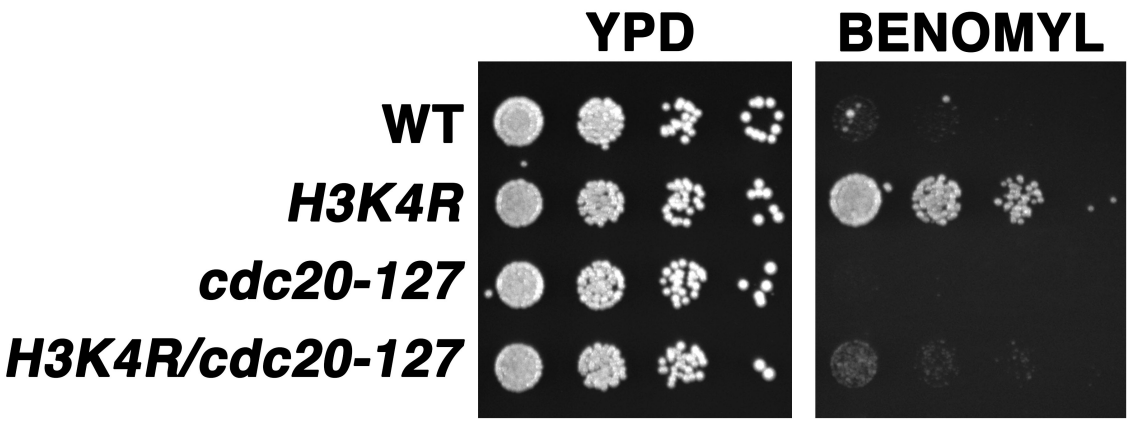

Figure 24

SAC components and Cdc20 bind directly to histone H3.

Methylation of H3K4 can directly affect binding of other proteins to chromatin, and several H3K4me reader domains have been identified, including WD40 repeats (Wysocka et al, 2005). Interestingly, both *BUB3* and *CDC20* contain multiple WD40 repeats. In addition, Mad2 contains a HORMA domain, which is found in multiple chromatin-associated proteins (Figure 25) (Aravind and Koonin, 1998; Muniyappa et al., 2014). To test whether any components of the SAC or Cdc20 bind directly to histones, we performed GST pull down experiments using recombinant, N-terminally tagged GST fusion proteins expressed in *E. coli* together with total calf thymus histones. We have found that GST-Bub3, GST-Cdc20, and GST-Mad2 all directly bind histone H3 but not H2A and H2B (Figure 26).

The WD40 repeats in Cdc20 are located in the C-terminal portion of the protein. To verify that these repeats are sufficient for direct binding of Cdc20 to histone H3, we expressed and purified a construct lacking the N-terminal portion of the protein. In addition, we expressed a version of GST-WD40 fusion protein that contains the G544R mutation encoded in the *cdc20-1* allele that exhibits limited functions *in vivo* (Sethi et al., 1991). The WD40 repeats in Cdc20 recruit substrates to the APC by binding to KEN and D-box motifs within the substrates (Chao et al., 2012; Tian et al., 2012). Here we show that the Cdc20 WD40 repeats also directly bind to histone H3, but not to H2A and H2B, and that the G544R mutation abolishes H3 binding (Figure 27).

Figure 25: An illustration of the domains present in Bub3, Cdc20, and Mad2

Bub3 and Cdc20 contain multiple WD40 domain repeats while Mad2 contains a HORMA domain.

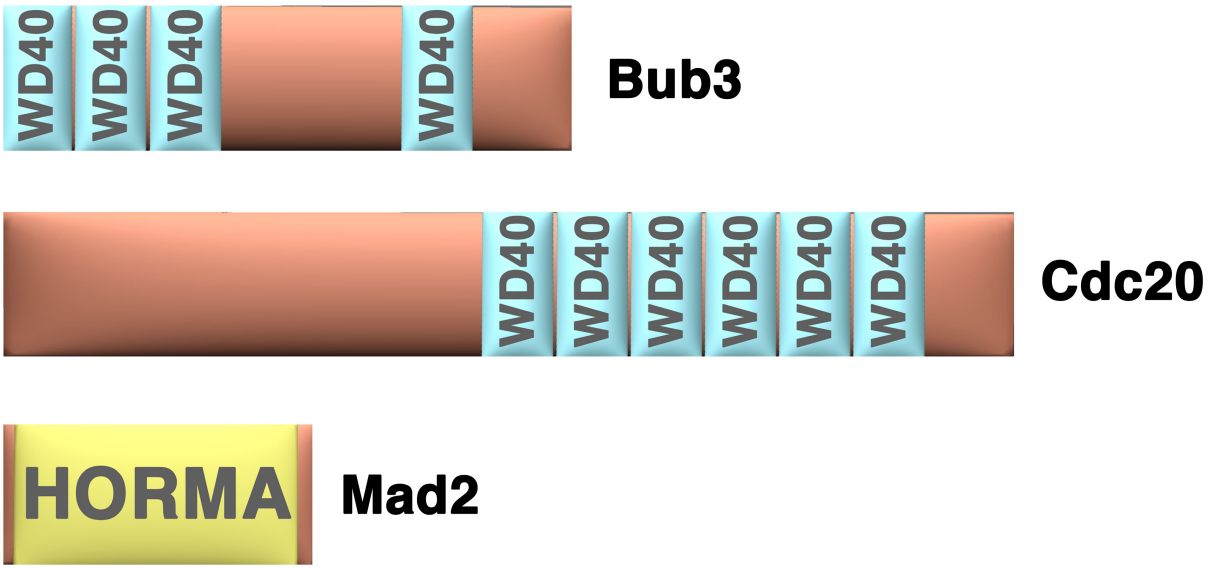
WD40
WD40
WD40
WD40
Bub3
WD40
WD40
WD40
WD40
WD40
WD40
Cdc20
HORMA
Mad2

Figure 25

Figure 26: Bub3, Cdc20, and Mad2 all directly bind histone H3

Colloidal staining of purified recombinant proteins. Pull down assays of GST-Bub3, GST-Cdc20, and GST-Mad2 to identify direct binding with histones isolated from calf thymus. Direct binding was assayed using immunoblots of membranes probed with antibodies against H2A, H2B or H3.

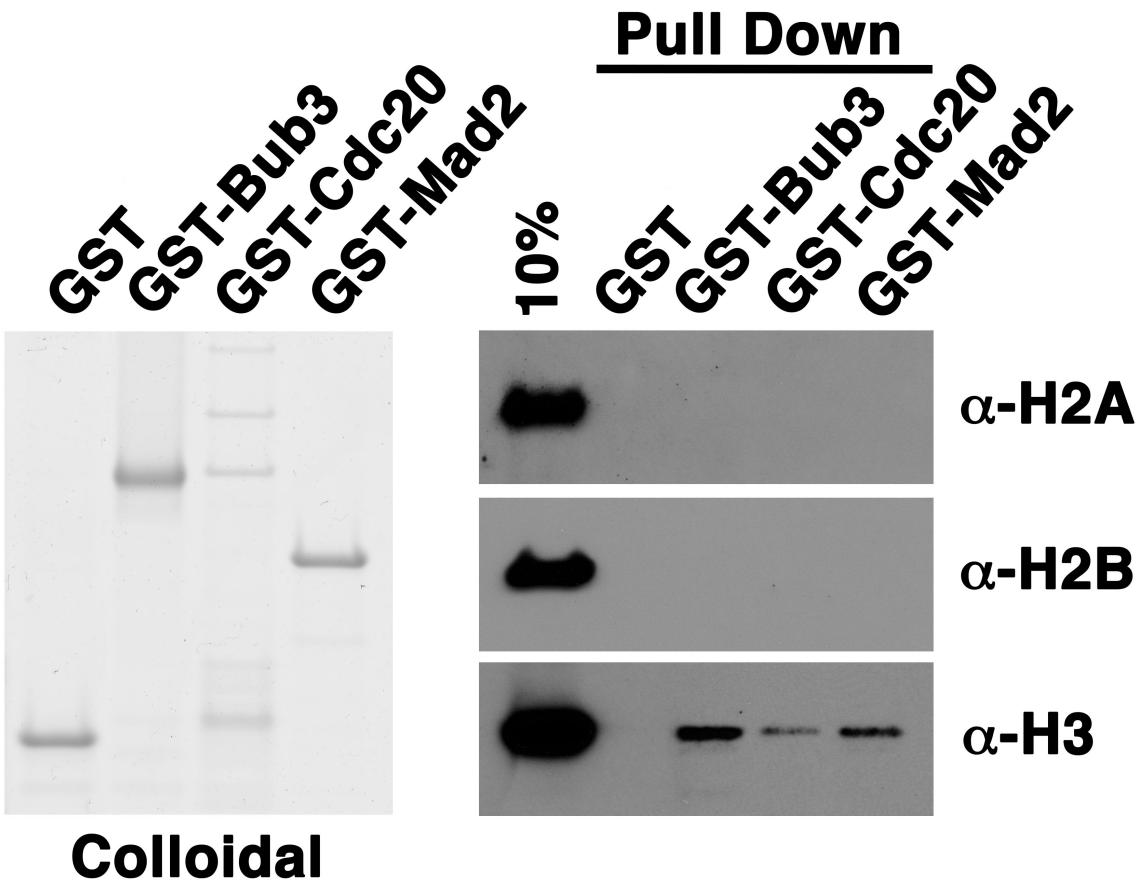
Pull Down
GST
GST-Bub3
GST-Cdc20
GST-Mad2
10%
GST
GST-Bub3
GST-Cdc20
GST-Mad2
α-H2A
α-H2B
α-H3
Colloidal

Figure 26

Figure 27: The WD40 repeats of Cdc20 are sufficient to bind H3.

Colloidal staining of purified recombinant proteins. Pull down assays of the WD40 domain of Cdc20 (GST-WD40) and with a point mutant (GST-WD40-G544R) to identify direct binding with histones isolated from calf thymus. Direct binding was assayed using immunoblots of membranes probed with antibodies against H2A, H2B or H3.

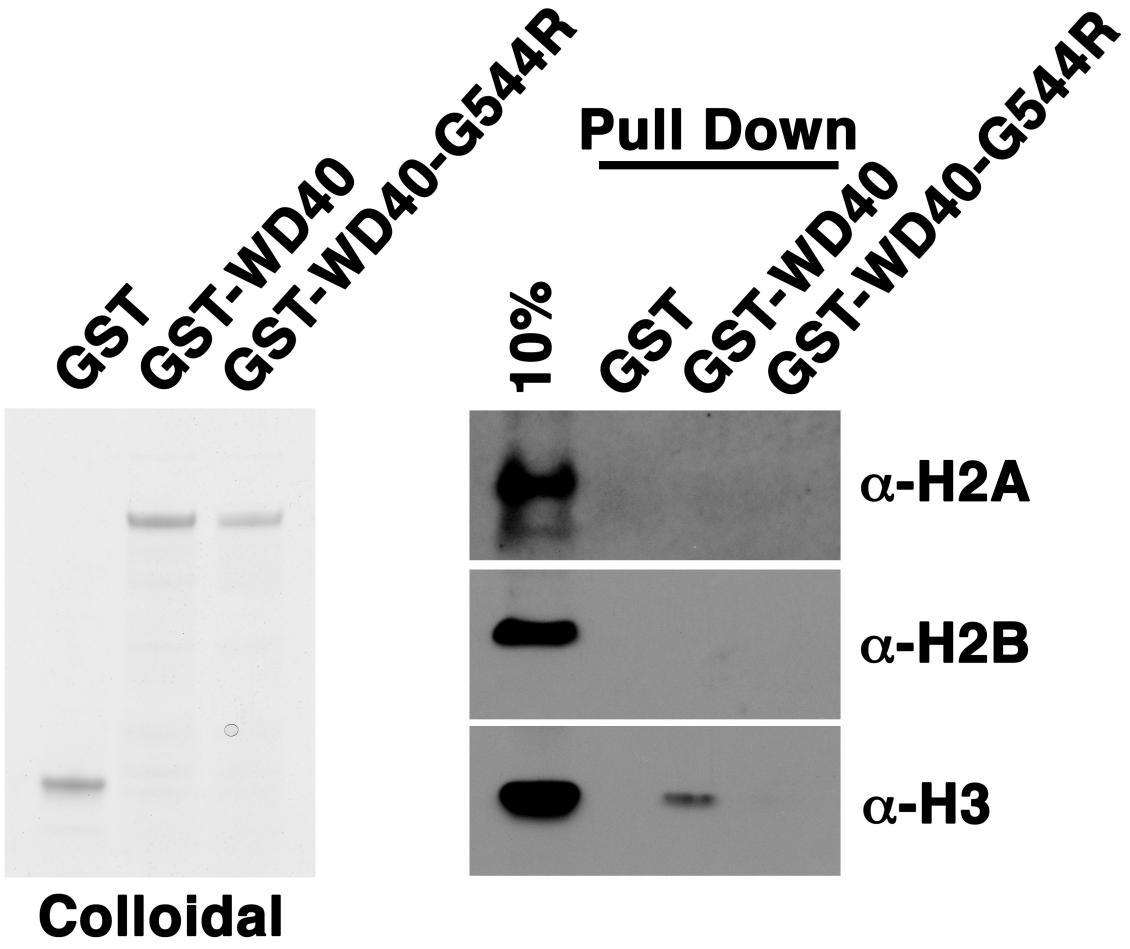
GST
GST-WD40
GST-WD40-G544R
Colloidal
Pull Down
10%
GST
GST-WD40
GST-WD40-G544R
α-H2A
α-H2B
α-H3

Figure 27

Figure 28: Cdc20 can bind all H3K4 methylation states

Pull down assay with recombinant GST fusion proteins and unmodified H3 (K4 me0) or MLA full length histones generated to mimic H3K4 monomethylation (K4 me1), H3K4 dimethylation (K4 me2) or H3K4 trimethylation (K4 me3). Direct binding was assayed using immunoblots of membranes probed with an antibody recognizing histone H3.

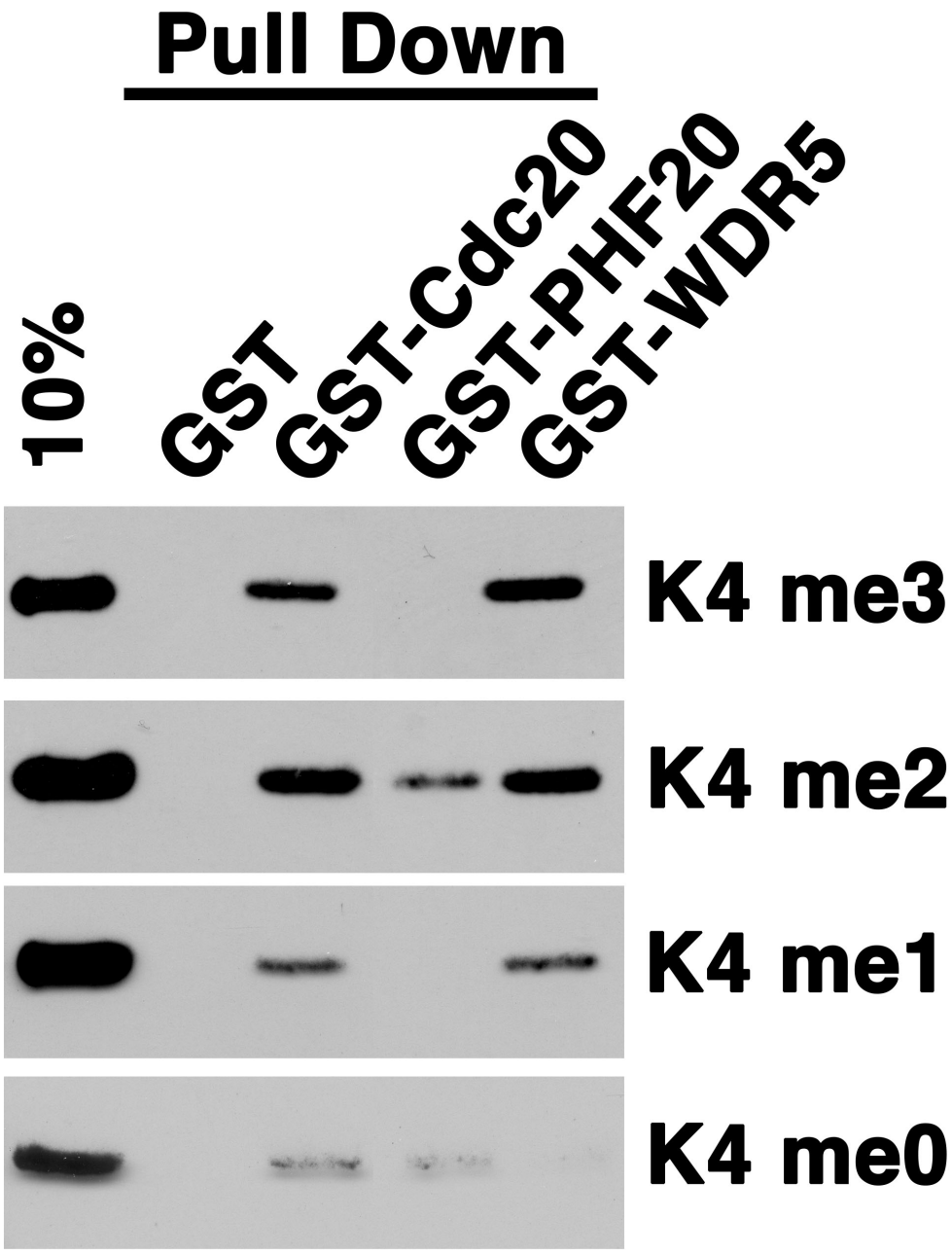
Pull Down
10%
GST
GST-Cdc20
GST-PHF20
GST-WDR5
K4 me3
K4 me2
K4 me1
K4 me0

Figure 28

Figure 29: Bub3 can bind all H3K4 methylation states

Pull down assay with recombinant GST fusion proteins and unmodified H3 (K4 me0) or MLA full length histones generated to mimic H3K4 monomethylation (K4 me1), H3K4 dimethylation (K4 me2) or H3K4 trimethylation (K4 me3). Direct binding was assayed using immunoblots of membranes probed with an antibody recognizing histone H3.

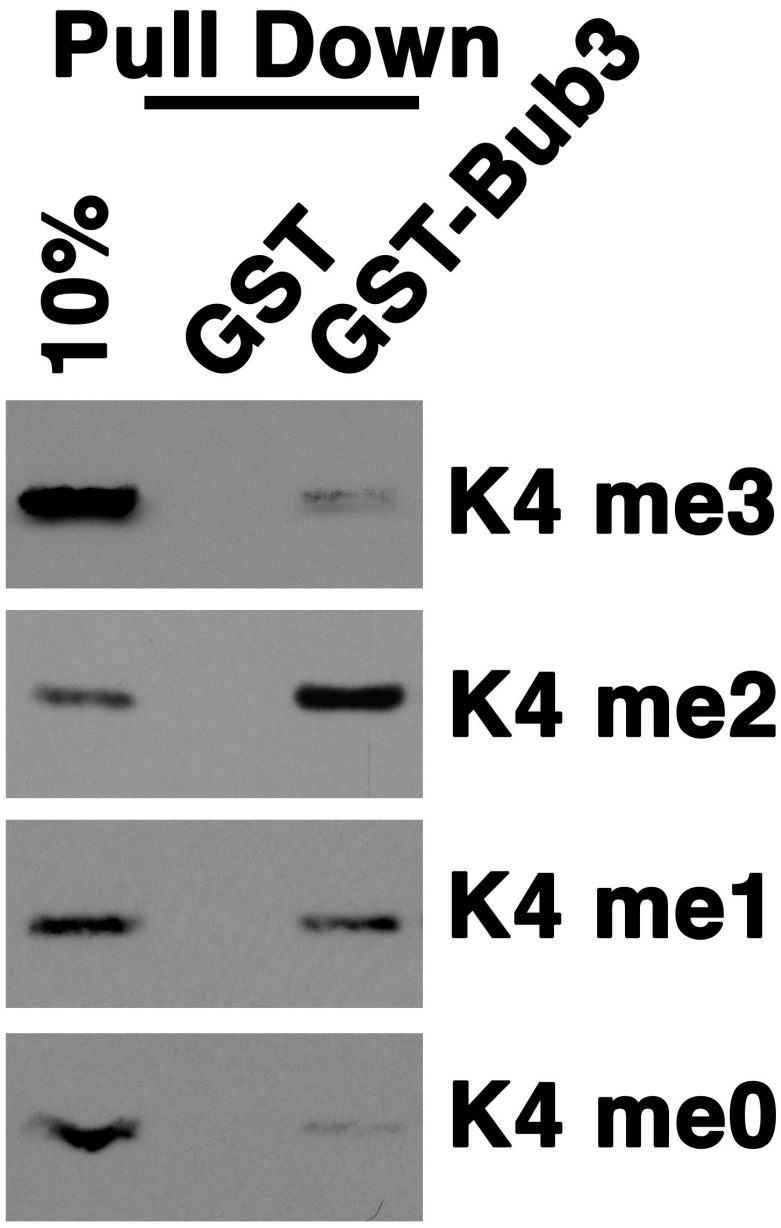

Figure 29

To address whether binding of Cdc20 or Bub3 to H3 is affected by K4 methylation, we repeated the GST pull down experiments using H3 bearing specific methylation states created by (MLA) modifications. Both GST-Cdc20 and GST-Bub3 interacted with histone H3 regardless of the methylation status of K4 (Figure 28 and 29).

Mad2 can adopt two conformational forms, Open Mad2 (O-Mad2) and Closed Mad2 (C-Mad2), in both yeast and humans (Luo et al., 2000; Nezi et al., 2006; Sironi et al., 2002). Specific mutations can structurally constrain Mad2 to either the O-Mad2 or the C-Mad2 conformation (De Antoni et al., 2005; Nezi et al., 2006). To determine whether Mad2 conformation affects binding to histone H3, we created GST versions of the O-Mad2 and C-Mad2 proteins and compared binding of these conformational states to that of wild-type Mad2. O-Mad2 interacted less well with histone H3 relative to wild-type Mad2. In contrast, C-Mad2 pulled down more histone H3 than did either the wild-type or O-Mad2 conformations. None of the Mad2 proteins bound to histone H2A or H2B, confirming specificity for H3 interactions (Figure 30).

In contrast to the inability of Bub3 or Cdc20 to discriminate between different methylation states of H3, O-Mad2 and C-Mad2 displayed strikingly different binding profiles to modified and unmodified forms of H3. C-Mad2 clearly bound to all methylation states of histone H3, whereas O-Mad2 bound best to H3K4me0 and displayed limited interaction with H3K4me1 (Figure 31). These findings identify Mad2 as a novel histone binding protein with conformation sensitive lysine methyl “reader” capability.

Figure 30: C-Mad2 directly binds H3

Colloidal staining of purified recombinant proteins. Pull down assays of the WD40 domain of Cdc20 (GST-WD40) and with a point mutant (GST-WD40-G544R) to identify direct binding with histones isolated from calf thymus. Direct binding was assayed using immunoblots of membranes probed with antibodies against H2A, H2B or H3.

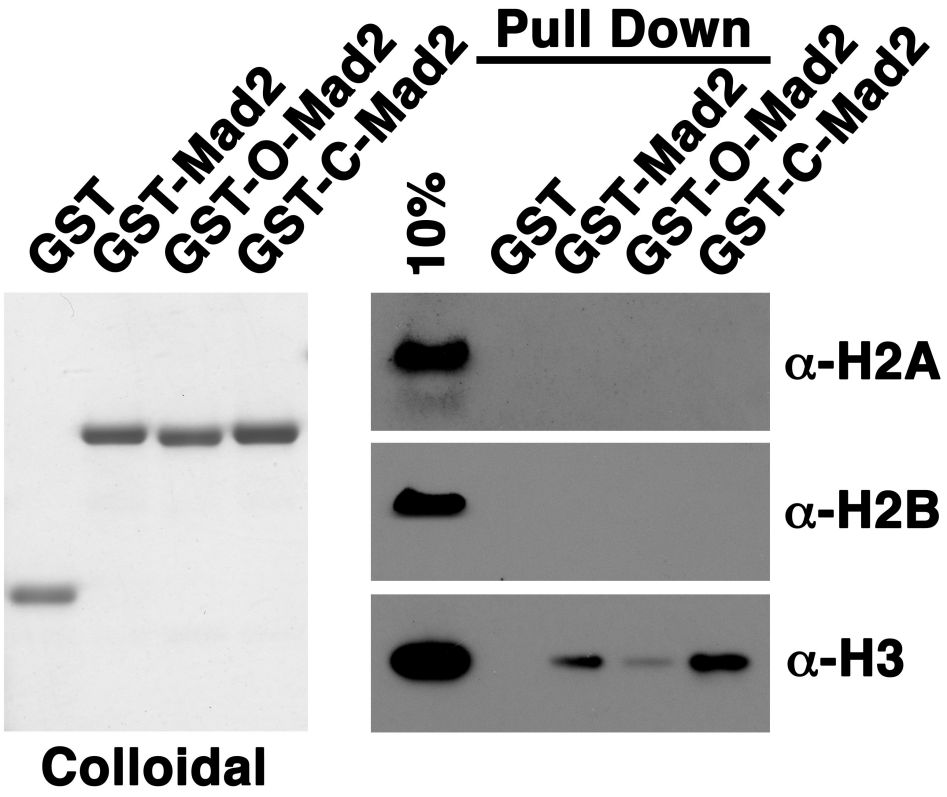
Pull Down
GST
GST-Mad2
GST-O-Mad2
GST-C-Mad2
10%
GST
GST-Mad2
GST-O-Mad2
GST-C-Mad2
α-H2A
α-H2B
α-H3
Colloidal

Figure 30

Figure 31: O-Mad2 binding is inhibited by H3K4 di- and tri-methylation

Pull down assay with recombinant GST fusion proteins and unmodified H3 (K4 me0) or MLA full length histones generated to mimic H3K4 monomethylation (K4 me1), H3K4 dimethylation (K4 me2) or H3K4 trimethylation (K4 me3). Direct binding was assayed using immunoblots of membranes probed with an antibody recognizing histone H3.

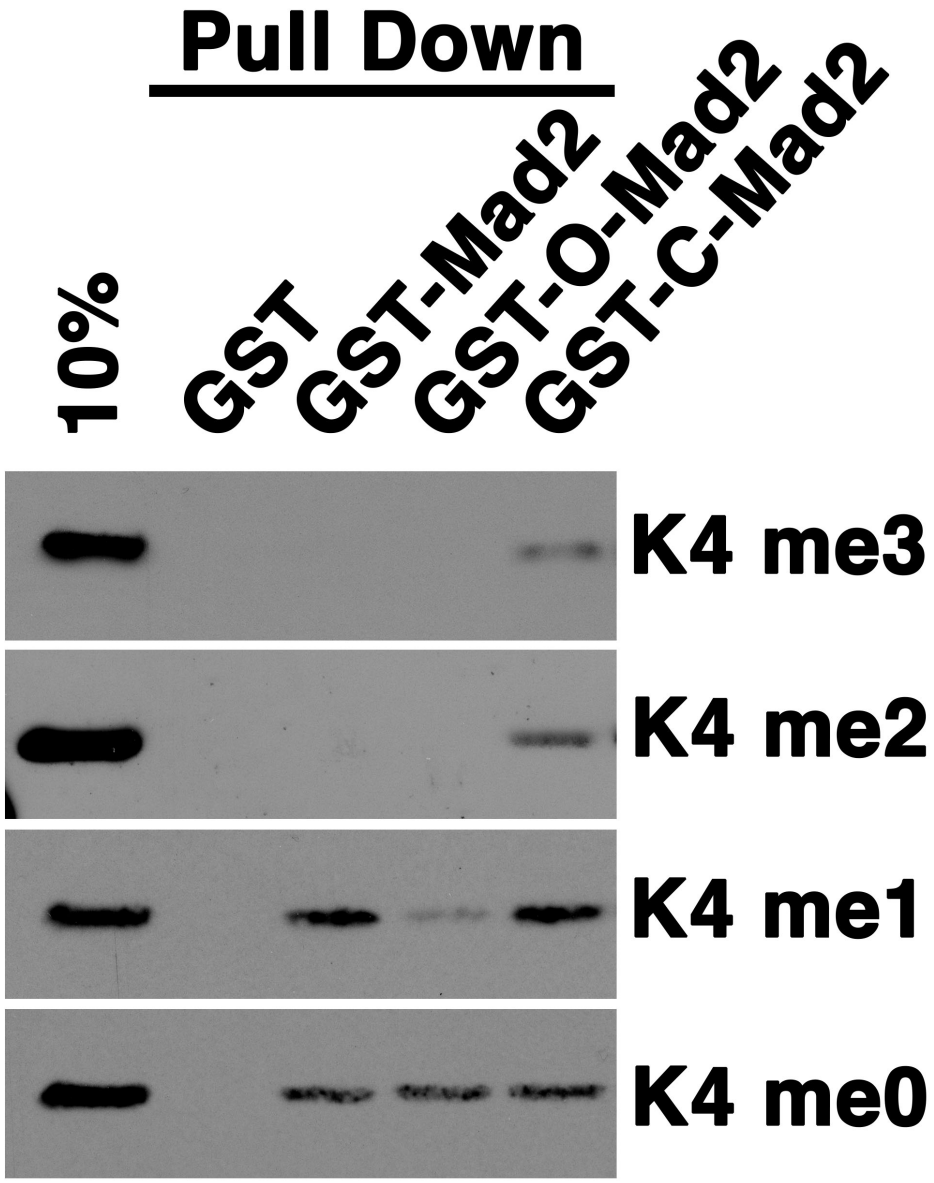
Pull Down
10%
GST
GST-Mad2
GST-O-Mad2
GST-C-Mad2
K4 me3
K4 me2
K4 me1
K4 me0

Figure 31

Chapter 4: Discussion

In this study we report Set1 is required to properly silence the SAC through H3K4 methylation, which in turn limits a novel histone H3-Mad2 protein interaction. To come to this conclusion, we identified a unique benomyl resistance phenotype displayed by a number of mutants limiting H3K4 methylation. Previous research identified that the SAC pathway is engaged in response to microtubule poisons, therefore we wanted to test if *H3K4R* mutants affect the SAC pathway resulting in a benomyl resistance phenotype. To do this, we generated multiple mutations abolishing the SAC and these assays revealed loss of H3K4 methylation results in an overactive SAC, which is functioning through Cdc20 inhibition.

A major function of H3K4 methylation is to recruit or exclude protein-protein interactions. Our initial results indicate that loss of H3K4 methylation is affecting SAC function. Therefore we wanted to test if any SAC components have the ability to bind directly to histone H3. Interestingly, we found Bub3, Cdc20, and Mad2 directly bind to histone H3. To investigate if Mad2 could bind to methylated H3K4 we introduced mutations to create two differing conformations of Mad2, termed O-Mad2 and C-Mad2. We tested the binding ability of both conformations to histones modified on H3K4 and found that H3K4 methylation blocked the binding of O-Mad2 but bound C-Mad2, indicating a conformational change has the ability to facilitate H3-protein interactions and this is mediated through H3K4 lysine methylation. These data suggest H3 and H3K4 methylation facilitate the SAC by promoting or excluding protein-protein

interactions of differing Mad2 conformations. Importantly, we also identified the HORMA domain as a novel histone binding motif and Mad2 as a histone H3K4 methyl reader regulated by a change in conformation. These data point to a previously unknown mechanism for mitotic checkpoint regulation through PTMs made to histone H3 coupled with a conformational change to Mad2.

We have shown C-Mad2 specifically bound di-methylated and tri-methylated histone H3K4 while the O-Mad2 could not. The mechanism by which C-Mad2 and O-Mad2 function as a reader of differing histone H3K4 methylation states needs further investigation. Other regulators of the SAC have been identified that directly interact with C-Mad2 but not O-Mad2. H3K4 methylation could function by specifically binding to C-Mad2 thereby blocking the dimerization of O-Mad2 and C-Mad2, an important regulatory event in SAC activation and maintenance (Habu et al., 2002; Mapelli et al., 2006; Xia et al., 2004). Histone H3K4 di- and tri-methylation could function as a conformation specific binder of C-Mad2 which would function to exclude O-Mad2. Lack of histone H3K4 methylation could result in uninhibited C-Mad2 and an increased suppression of Cdc20 function (Figure 32).

We have *in vitro* experiments showing histone H3K4 methylation regulates Mad2-H3 protein interactions and we have *in vivo* data suggesting H3K4 methylation limits the SAC pathway. Previous studies have identified another silencing factor of the SAC named P31^{comet}, which shares many similarities with methylated histone H3K4. P31^{comet}

Figure 32: A model of APC inhibition by Mad2 in wild-type and mutant cells

An illustration of the SAC in both wild-type (WT) and *set1* mutant cells (Set1 Mutant). In wild-type cells, dimethylation of H3K4 (H3K4me2) specifically binds Closed Mad2 (C-Mad2) which inhibits the interaction of Open Mad2 (O-Mad2) with C-Mad2 a regulatory step required for continued inhibition of the SAC. After SAC activation, H3K4me2 acts as a limiting factor by binding C-Mad2. In wild-type cells, the APC bound by Cdc20 is then able to ubiquitinate substrates such as Pds1 (Securin). In the *H3K4R* mutants, O-Mad2 is not inhibited by dimethylation of H3K4 and can associate with C-Mad2 leading to continued inhibition of the SAC and Pds1 stability after tension is established.

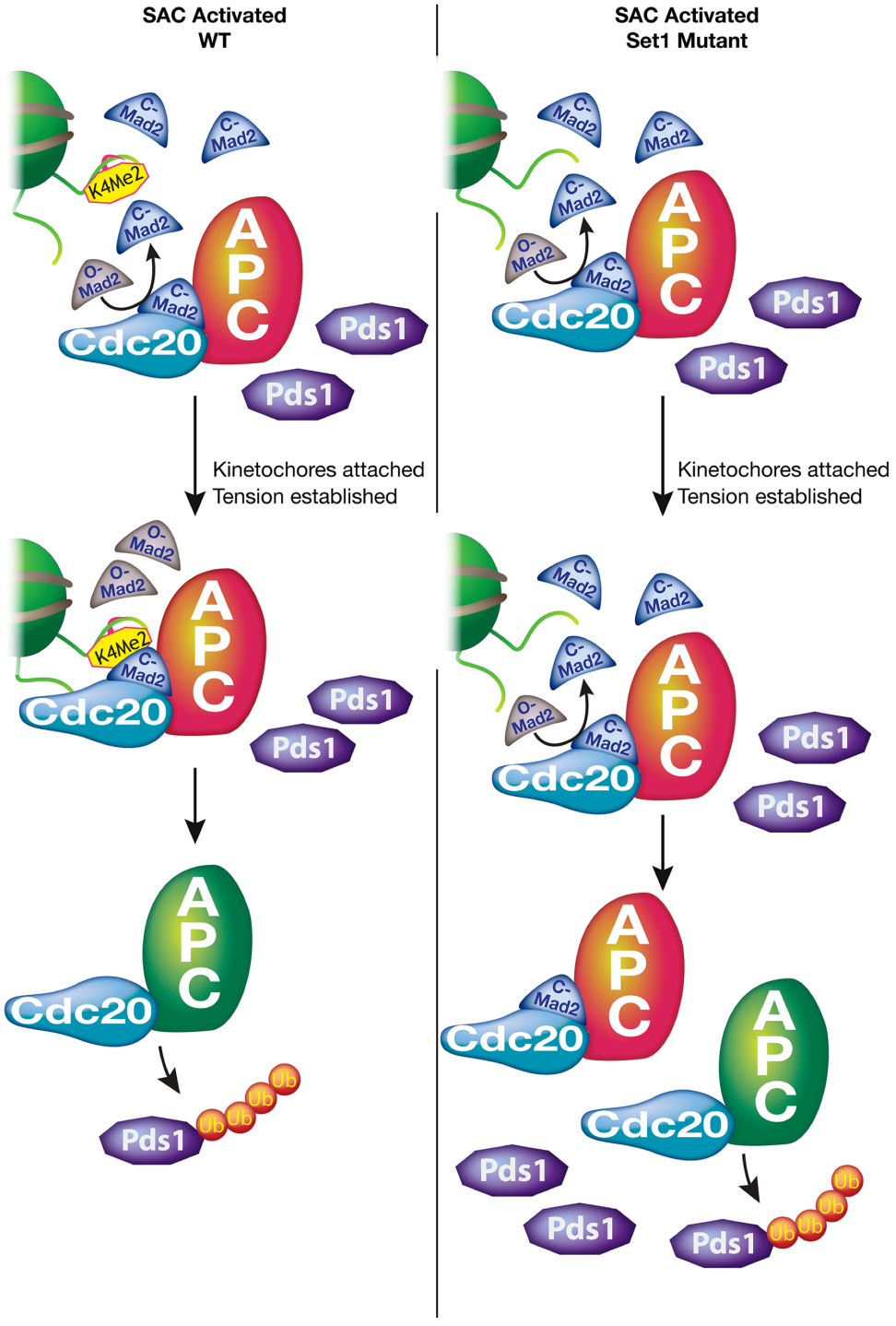
SAC Activated
WT
SAC Activated
Set1 Mutant
C-Mad2
O-Mad2
K4Me2
APC
Cdc20
Pds1
Ub
Kinetochores attached
Tension established

Figure 32

was first identified with a yeast two-hybrid experiment in which human Mad2 was used as bait suggesting a direct P31^{comet}-Mad2 interaction, much like our findings with Mad2 and H3. Subsequent experiments indicated that overexpressing P31^{comet} while the SAC was active resulted in cells that continue through the cell cycle adopting an aneuploid phenotype. Next, cells depleted of P31^{comet} were arrested by activating the SAC and released into fresh media, cells lacking P31^{comet} maintained an increased number of cells that remained in metaphase compared to control cells. These data suggest overexpressing P31^{comet} silences the SAC while restricting P31^{comet} creates cells deficient in SAC deactivation. We performed similar *in vivo* experiments and much like P31^{comet}, cells lacking H3K4 methylation activated the SAC but did not properly release through the cell cycle suggesting a deficiency in silencing the SAC. Later studies found that P31^{comet} directly binds C-Mad2 but not O-Mad2, which is similar to what we discovered, in our studies methylated H3K4 bound C-Mad2 but not O-Mad2. In addition, previous research also found P31^{comet} bound C-Mad2 but did not interfere with the C-Mad2-Cdc20 interaction suggesting the relationship between P31^{comet}, C-Mad2, and Cdc20 was not mutually exclusive (Xia et al., 2004). Lastly, the crystal structure of p31^{comet} was resolved while associated with C-Mad2. This structure confirmed previous findings in which, p31^{comet} bound to Mad2 at a site away from the Cdc20 binding site. Lastly, this binding interface normally associates with Mad3 and also promotes the interaction between O-Mad2 and C-Mad2. Therefore the association of p31^{comet} with C-Mad2 would result in excluding Mad3 and O-Mad2 from association with the mitotic checkpoint complex (MCC) and antagonize the SAC (Chao et al., 2012).

Our studies identified the HORMA domain encoded by *MAD2* is a novel histone-binding motif with lysine methylation reading abilities. This creates the possibility that other HORMA domain containing proteins have the ability to read methylated histone marks. A number of other chromatin-associated proteins contain conserved HORMA domains in yeast and humans. These include human REV7, HORMAD1, HORMAD2, $p31^{comet}$, and MAD2. In addition, the yeast homologs containing HORMA domains are Rev7, Hop1, and Mad2.

Yeast and human REV7 are involved in DNA translesion synthesis and double strand break repair (Kolas and Durocher, 2006; Prakash et al., 2005). In addition, hREV7 is reported to bind and inhibit Cdh1, an ortholog of Cdc20, much like Mad2 (Listovsky and Sale, 2013). Although this interaction has not been reported in yeast, Cdh1 is also an activator of the APC through recruitment of substrates for ubiquitination and protein degradation. Like yeast and hMad2, hREV7 has been reported to undergo a conformational change upon binding to hREV1 (Hara et al., 2010). hREV7 has also been implicated in cancer. Triple negative breast cancer frequently loses hREV7 expression and this loss of hREV7 results in PARP inhibitor resistance (Xu et al., 2015).

Yeast Hop1 is a meiosis specific protein that is related to human meiosis proteins HORMAD1 and HORMAD2, which are paralogs. HORMAD proteins and histone H3K4 trimethylation have both been implicated in meiotic recombination (Handel and

Schimenti, 2010) although never molecularly connected. In addition, recent research found *C. elegans* Hop1 homologs could undergo a conformational change much like MAD2 and REV7 and identified conserved homologous sequences in HORMAD1 and HORMAD2 implicating a possibility for conformational change of all human HORMA domain-containing proteins (Kim et al., 2014). Lastly, in triple negative breast cancers, HORMAD1 overexpression has been implicated in deficient homologous recombination (Watkins et al., 2015). Due to the striking similarities between HORMA domain containing proteins, their association with chromatin, and their implications in human disease we propose an extensive study to characterize their association with histone H3. Further investigation is required to identify if HORMA domain containing proteins also specifically bind histone H3 in humans and in yeast, if a conformational change affects the binding, and if these interactions are either promoted or excluded by H3K4 methylation events.

Our data identifies a novel pathway showing how mutations to lysine methyltransferases and SAC components in yeast might contribute to cancer progression through loss of intricacies in mitotic checkpoint regulation in humans. The human homolog of yeast *SET1* is *MLL1*. *MLL1* is mutated in a subset of aggressive acute lymphoblastic leukemias (Guenther et al., 2005; Zeleznik-Le et al., 1994) possibly through misregulation of histone H3K4 methylation. We also reported yeast *BRE1* as being required for both H3K4 methylation events and a proper response to the microtubule poison, benomyl. Human BRE1 displays tumor suppressor features

(Shema et al., 2008) associated with lack of H2B ubiquitination and hBRE1 is frequently down regulated in metastatic prostate cancers (Varambally et al., 2005). It is important that future work identifies if proper SAC function is lost in cancers maintaining mutations either to *MLL1* or *BRE1*.

Interestingly, SAC components are often mutated or misregulated in cancer. Bub1 dominant negative mutations display a chromosomal instability (CIN) phenotype in colorectal cancer cell lines (Cahill et al., 1998) and mutations have been identified in many other cancer types (reviewed in (Fang and Zhang, 2011)). Additionally, although not directly mutated, the SAC pathway is repetitively attenuated by activators and repressors. For example, an increase in Mad2 is seen following Rb and p53 inhibition and reduction of Mad2 in these studies rescues the CIN observed in Rb and p53 deficient mice (Schvartzman et al., 2011). Lastly, Cdc20 is also overexpressed in a high percentage of colorectal and bladder cancer tissues and Cdc20 expression is repressed upon introduction of wild-type p53 expression (Kidokoro et al., 2008). These two studies link p53 inhibition to an aberrant SAC. p53 is mutated or deleted in over 50% of human tumors (Hollstein et al., 1991) suggesting an attenuated SAC pathway could play a substantial role in cancer initiation, maintenance, or progression.

Future Directions

Our findings indicate that Set1 negatively regulates the SAC through binding of histone H3 with Mad2. We additionally found Bub3 and Cdc20 also interact with H3 but in a manner independent of H3K4 methylation. Bub3 and Cdc20 can bind unmodified, mono-, di-, and tri-methylated histone H3K4. Although we identified these two proteins as novel histone H3 interacting proteins, we did not elucidate how the Bub3-H3 and Cdc20-H3 interactions are regulated or their function. It is likely that alternative histone H3 modifications either promote or inhibit the binding of Bub3 and Cdc20 to chromatin. By using our *in vitro* binding assays, we could identify histone marks excluding or promoting the binding of Bub3 and Cdc20 to H3. Further studies of the effect histone H3 has on the SAC pathway through Bub3 and Cdc20 would uncover additional regulatory events and implicate alternative PTMs in SAC regulation.

Another worthwhile experiment is to identify if hMAD2 can also bind histone H3 while it is in a closed conformation. We know histone H3K4 methylation is conserved between yeast and humans although we have not asked if hMAD2 maintains the ability to act as a lysine methyl reader. Mutations can be added into the hMAD2 sequence to lock MAD2 into either an O-MAD2 or a C-MAD2 conformation. Much like the studies we performed here, these H3-MAD2 interactions can be evaluated by using recombinant MAD2 and histone H3 to limit other PTMs. Similarly to the studies describing the $p31^{comet}$ –H3 interaction, we should also use protein crystallization to resolve the H3 C-Mad2 protein-protein interface. Identifying the binding surface of Mad2 with modified

H3 would facilitate in our understanding of SAC regulation. In addition, resolution of the C-Mad2 binding pocket that identifies and binds methylated H3 and how it changes when Mad2 is in an open conformation is crucial to our understanding of histone methyl readers and how Mad2 limits interactions with methylated binding partners due to a conformational change.

Histone H3K4 methylation is one of three H3 lysine methylation events in yeast. In addition, other lysine methylation events on histone H3 might serve to either promote or inhibit HORMA domain-histone H3 interactions. These include H3K36 and H3K79 mono-, di-, and tri-methylation. These interactions between H3 methylated at either K36 or K79 could easily be tested with our *in vitro* histone binding assays coupled with recombinant Bub3, Cdc20, and Mad2. Lastly, additional well-studied post-translational modifications of histone H3 such as H3S10 phosphorylation or H3K9 and K14 acetylation should also be introduced into our binding assays. Other histone modifications might also play a role in either promoting or inhibiting histone H3 interactions with Bub3, Cdc20, or Mad2. Further analysis of how histones interact with SAC components and Cdc20 is required to identify novel regulatory mechanisms identifying how SAC components directly bind to histone H3 and the downstream functions of these interactions.

Lastly, it would be informative to describe SAC-H3 interactions in time and space. SAC proteins have the ability to change their subcellular localization and associate with

multiple cellular structures including the nuclear envelope, both attached and unattached kinetochores, and the mitotic spindle. In addition, cell cycle changes and SAC activation have the ability to change SAC protein interactions. Identifying exactly when and where SAC proteins bind chromatin will be informative in understanding both chromatin and SAC regulatory events. Understanding if regulation is at the telomeres, centromeres, specific to certain genes, or dispersed throughout the genome will further identify how the genome is regulated throughout the cell cycle.

Significance

Here we show the first evidence of H3K4 methylation silencing the Spindle Assembly Checkpoint through direct interactions with C-Mad2. By using yeast as a model system combined with point mutations directly abolishing histone H3K4 methylation we were able to exclusively link loss of H3K4 methylation with a novel benomyl resistance phenotype. Through additional mutations introduce into the *H3K4R* mutant background we were able to further conclude loss of H3K4 methylation results in an overactive SAC that functions through Cdc20 inhibition. We then performed *in vitro* recombinant binding assays with MLA histones to extensively study how H3K4 methylation affects direct binding of Bub3, Cdc20, and Mad2 to histone H3. These binding studies identified novel H3 interacting proteins and a novel histone H3-binding motif, the HORMA domain. Lastly, a conformational change to C-Mad2 promotes Mad2-H3K4 methyl interactions, while the O-Mad2 conformation abolishes interactions with methylated

H3K4. These data suggest for the first time, a conformational change to the Mad2 protein produces a novel lysine methyl reader.

Our data links the SAC with histone H3K4 methylation thus uncovering a hidden regulatory event required for proper cell division. Histone H3K4 methylation and the SAC are highly conserved and attenuation of either histone modifications or the SAC is associated with cancer. A further understanding of how H3K4 methylation and SAC inhibition contribute to cellular regulatory events will help us to better understand cancer progression and human disease. Lastly, our approach using yeast genetics and cell biology assays coupled with *in vitro* binding assays led to a conclusive approach to find novel SAC activators and inhibitors, suggesting further experiments will identify additional regulators of cell division through post translational modifications and possibly histone H3.

Bibliography

Aravind, L., and Koonin, E.V. (1998). The HORMA domain: a common structural denominator in mitotic checkpoints, chromosome synapsis and DNA repair. Trends in Biochemical Sciences *23*, 284-286.

Badis, G., Chan, E.T., van Bakel, H., Pena-Castillo, L., Tillo, D., Tsui, K., Carlson, C.D., Gossett, A.J., Hasinoff, M.J., Warren, C.L.*, et al.* (2008). A library of yeast transcription factor motifs reveals a widespread function for Rsc3 in targeting nucleosome exclusion at promoters. Molecular Cell *32*, 878-887.

Bannister, A.J., Zegerman, P., Partridge, J.F., Miska, E.A., Thomas, J.O., Allshire, R.C., and Kouzarides, T. (2001). Selective recognition of methylated lysine 9 on histone H3 by the HP1 chromo domain. Nature *410*, 120-124.

Bernstein, B.E., Humphrey, E.L., Erlich, R.L., Schneider, R., Bouman, P., Liu, J.S., Kouzarides, T., and Schreiber, S.L. (2002). Methylation of histone H3 Lys 4 in coding regions of active genes. Proceedings of the National Academy of Sciences of the United States of America *99*, 8695-8700.

Bernstein, B.E., Liu, C.L., Humphrey, E.L., Perlstein, E.O., and Schreiber, S.L. (2004). Global nucleosome occupancy in yeast. Genome Biology *5*, R62.

Biggins, S., and Murray, A.W. (2001). The budding yeast protein kinase Ipl1/Aurora allows the absence of tension to activate the spindle checkpoint. Genes & Development *15*, 3118-3129.

Biggins, S., Severin, F.F., Bhalla, N., Sassoon, I., Hyman, A.A., and Murray, A.W. (1999). The conserved protein kinase Ipl1 regulates microtubule binding to kinetochores in budding yeast. Genes & Development *13*, 532-544.

Briggs, S.D., Bryk, M., Strahl, B.D., Cheung, W.L., Davie, J.K., Dent, S.Y., Winston, F., and Allis, C.D. (2001). Histone H3 lysine 4 methylation is mediated by Set1 and required for cell growth and rDNA silencing in Saccharomyces cerevisiae. Genes & Development *15*, 3286-3295.

Burke, D., Dawson, D., Stearns, T., and Cold Spring Harbor Laboratory. (2000). Methods in yeast genetics : a Cold Spring Harbor Laboratory Course Manual, 2000 edn (Plainview, N.Y.: Cold Spring Harbor Laboratory Press).

Buvelot, S., Tatsutani, S.Y., Vermaak, D., and Biggins, S. (2003). The budding yeast Ipl1/Aurora protein kinase regulates mitotic spindle disassembly. The Journal of Cell Biology *160*, 329-339.

Cahill, D.P., Lengauer, C., Yu, J., Riggins, G.J., Willson, J.K., Markowitz, S.D., Kinzler, K.W., and Vogelstein, B. (1998). Mutations of mitotic checkpoint genes in human cancers. Nature *392*, 300-303.

Cairns, B.R., Lorch, Y., Li, Y., Zhang, M., Lacomis, L., Erdjument-Bromage, H., Tempst, P., Du, J., Laurent, B., and Kornberg, R.D. (1996). RSC, an essential, abundant chromatin-remodeling complex. Cell *87*, 1249-1260.

Chai, B., Huang, J., Cairns, B.R., and Laurent, B.C. (2005). Distinct roles for the RSC and Swi/Snf ATP-dependent chromatin remodelers in DNA double-strand break repair. Genes & Development *19*, 1656-1661.

Chao, W.C., Kulkarni, K., Zhang, Z., Kong, E.H., and Barford, D. (2012). Structure of the mitotic checkpoint complex. Nature *484*, 208-213.

Cheeseman, I.M., Anderson, S., Jwa, M., Green, E.M., Kang, J., Yates, J.R., 3rd, Chan, C.S., Drubin, D.G., and Barnes, G. (2002). Phospho-regulation of kinetochore-microtubule attachments by the Aurora kinase Ipl1p. Cell *111*, 163-172.

Chen, L., Trujillo, K., Ramos, W., Sung, P., and Tomkinson, A.E. (2001). Promotion of Dnl4-catalyzed DNA end-joining by the Rad50/Mre11/Xrs2 and Hdf1/Hdf2 complexes. Molecular Cell *8*, 1105-1115.

De Antoni, A., Pearson, C.G., Cimini, D., Canman, J.C., Sala, V., Nezi, L., Mapelli, M., Sironi, L., Faretta, M., Salmon, E.D.*, et al.* (2005). The Mad1/Mad2 complex as a template for Mad2 activation in the spindle assembly checkpoint. Current Biology : CB *15*, 214-225.

Dehe, P.M., Pamblanco, M., Luciano, P., Lebrun, R., Moinier, D., Sendra, R., Verreault, A., Tordera, V., and Geli, V. (2005). Histone H3 lysine 4 mono-methylation does not require ubiquitination of histone H2B. Journal of Molecular Biology *353*, 477-484.

Fang, X., and Zhang, P. (2011). Aneuploidy and tumorigenesis. Seminars in Cell & Developmental Biology *22*, 595-601.

Gale, J.M., Nissen, K.A., and Smerdon, M.J. (1987). UV-induced formation of pyrimidine dimers in nucleosome core DNA is strongly modulated with a period of 10.3 bases. Proceedings of the National Academy of Sciences of the United States of America *84*, 6644-6648.

Ganapathi, M., Palumbo, M.J., Ansari, S.A., He, Q., Tsui, K., Nislow, C., and Morse, R.H. (2011). Extensive role of the general regulatory factors, Abf1 and Rap1, in determining genome-wide chromatin structure in budding yeast. Nucleic Acids Research *39*, 2032-2044.

Garcia, B.A., Hake, S.B., Diaz, R.L., Kauer, M., Morris, S.A., Recht, J., Shabanowitz, J., Mishra, N., Strahl, B.D., Allis, C.D.*, et al.* (2007). Organismal differences in post-translational modifications in histones H3 and H4. The Journal of Biological Chemistry *282*, 7641-7655.

Gillett, E.S., Espelin, C.W., and Sorger, P.K. (2004). Spindle checkpoint proteins and chromosome-microtubule attachment in budding yeast. The Journal of Cell Biology *164*, 535-546.

Gong, F., Fahy, D., and Smerdon, M.J. (2006). Rad4-Rad23 interaction with SWI/SNF links ATP-dependent chromatin remodeling with nucleotide excision repair. Nature Structural & Molecular Biology *13*, 902-907.

Groth, A., Corpet, A., Cook, A.J., Roche, D., Bartek, J., Lukas, J., and Almouzni, G. (2007). Regulation of replication fork progression through histone supply and demand. Science *318*, 1928-1931.

Guenther, M.G., Jenner, R.G., Chevalier, B., Nakamura, T., Croce, C.M., Canaani, E., and Young, R.A. (2005). Global and Hox-specific roles for the MLL1 methyltransferase. Proceedings of the National Academy of Sciences of the United States of America *102*, 8603-8608.

Habu, T., Kim, S.H., Weinstein, J., and Matsumoto, T. (2002). Identification of a MAD2-binding protein, CMT2, and its role in mitosis. The EMBO Journal *21*, 6419-6428.

Handel, M.A., and Schimenti, J.C. (2010). Genetics of mammalian meiosis: regulation, dynamics and impact on fertility. Nature Reviews Genetics *11*, 124-136.

Hara, K., Hashimoto, H., Murakumo, Y., Kobayashi, S., Kogame, T., Unzai, S., Akashi, S., Takeda, S., Shimizu, T., and Sato, M. (2010). Crystal structure of human REV7 in complex with a human REV3 fragment and structural implication of the interaction between DNA polymerase zeta and REV1. The Journal of Biological Chemistry *285*, 12299-12307.

Hirschhorn, J.N., Brown, S.A., Clark, C.D., and Winston, F. (1992). Evidence that SNF2/SWI2 and SNF5 activate transcription in yeast by altering chromatin structure. Genes & Development *6*, 2288-2298.

Hollstein, M., Sidransky, D., Vogelstein, B., and Harris, C.C. (1991). p53 mutations in human cancers. Science *253*, 49-53.

Hoyt, M.A., Totis, L., and Roberts, B.T. (1991). S. cerevisiae genes required for cell cycle arrest in response to loss of microtubule function. Cell *66*, 507-517.

Iouk, T., Kerscher, O., Scott, R.J., Basrai, M.A., and Wozniak, R.W. (2002). The yeast nuclear pore complex functionally interacts with components of the spindle assembly checkpoint. The Journal of Cell Biology *159*, 807-819.

Jansen, L.E., Verhage, R.A., and Brouwer, J. (1998). Preferential binding of yeast Rad4.Rad23 complex to damaged DNA. The Journal of Biological Chemistry *273*, 33111-33114.

Kidokoro, T., Tanikawa, C., Furukawa, Y., Katagiri, T., Nakamura, Y., and Matsuda, K. (2008). CDC20, a potential cancer therapeutic target, is negatively regulated by p53. Oncogene *27*, 1562-1571.

Kim, J., Daniel, J., Espejo, A., Lake, A., Krishna, M., Xia, L., Zhang, Y., and Bedford, M.T. (2006). Tudor, MBT and chromo domains gauge the degree of lysine methylation. EMBO Reports *7*, 397-403.

Kim, Y., Rosenberg, S.C., Kugel, C.L., Kostow, N., Rog, O., Davydov, V., Su, T.Y., Dernburg, A.F., and Corbett, K.D. (2014). The chromosome axis controls meiotic events through a hierarchical assembly of HORMA domain proteins. Developmental Cell *31*, 487-502.

Kolas, N.K., and Durocher, D. (2006). DNA repair: DNA polymerase zeta and Rev1 break in. Current Biology : CB *16*, R296-299.

Krogan, N.J., Dover, J., Khorrami, S., Greenblatt, J.F., Schneider, J., Johnston, M., and Shilatifard, A. (2002). COMPASS, a histone H3 (Lysine 4) methyltransferase required for telomeric silencing of gene expression. The Journal of Biological Chemistry *277*, 10753-10755.

Krogan, N.J., Dover, J., Wood, A., Schneider, J., Heidt, J., Boateng, M.A., Dean, K., Ryan, O.W., Golshani, A., Johnston, M.*, et al.* (2003). The Paf1 complex is required for histone H3 methylation by COMPASS and Dot1p: linking transcriptional elongation to histone methylation. Molecular Cell *11*, 721-729.

Latham, J.A., Chosed, R.J., Wang, S., and Dent, S.Y. (2011). Chromatin signaling to kinetochores: transregulation of Dam1 methylation by histone H2B ubiquitination. Cell *146*, 709-719.

Lee, J.S., Shukla, A., Schneider, J., Swanson, S.K., Washburn, M.P., Florens, L., Bhaumik, S.R., and Shilatifard, A. (2007a). Histone crosstalk between H2B monoubiquitination and H3 methylation mediated by COMPASS. Cell *131*, 1084-1096.

Lee, W., Tillo, D., Bray, N., Morse, R.H., Davis, R.W., Hughes, T.R., and Nislow, C. (2007b). A high-resolution atlas of nucleosome occupancy in yeast. Nature Genetics *39*, 1235-1244.

Li, R., and Murray, A.W. (1991). Feedback control of mitosis in budding yeast. Cell *66*, 519-531.

Li, S. (2012). Implication of posttranslational histone modifications in nucleotide excision repair. International Journal of Molecular Sciences *13*, 12461-12486.

Li, X., and Nicklas, R.B. (1995). Mitotic forces control a cell-cycle checkpoint. Nature *373*, 630-632.

Lipford, J.R., and Bell, S.P. (2001). Nucleosomes positioned by ORC facilitate the initiation of DNA replication. Molecular Cell *7*, 21-30.

Listovsky, T., and Sale, J.E. (2013). Sequestration of CDH1 by MAD2L2 prevents premature
APC/C activation prior to anaphase onset. The Journal of Cell Biology *203*, 87-100.

Luger, K., Mader, A.W., Richmond, R.K., Sargent, D.F., and Richmond, T.J. (1997). Crystal structure of the nucleosome core particle at 2.8 A resolution. Nature *389*, 251-260.

Luo, X., Fang, G., Coldiron, M., Lin, Y., Yu, H., Kirschner, M.W., and Wagner, G. (2000). Structure of the Mad2 spindle assembly checkpoint protein and its interaction with Cdc20. Nature Structural Biology *7*, 224-229.

Mapelli, M., Filipp, F.V., Rancati, G., Massimiliano, L., Nezi, L., Stier, G., Hagan, R.S., Confalonieri, S., Piatti, S., Sattler, M.*, et al.* (2006). Determinants of conformational dimerization of Mad2 and its inhibition by p31comet. The EMBO Journal *25*, 1273-1284.

Matallana, E., Franco, L., and Perez-Ortin, J.E. (1992). Chromatin structure of the yeast SUC2 promoter in regulatory mutants. Molecular & General Genetics : MGG *231*, 395-400.

Mavrich, T.N., Ioshikhes, I.P., Venters, B.J., Jiang, C., Tomsho, L.P., Qi, J., Schuster, S.C., Albert, I., and Pugh, B.F. (2008). A barrier nucleosome model for statistical positioning of nucleosomes throughout the yeast genome. Genome Research *18*, 1073-1083.

Miller, T., Krogan, N.J., Dover, J., Erdjument-Bromage, H., Tempst, P., Johnston, M., Greenblatt, J.F., and Shilatifard, A. (2001). COMPASS: a complex of proteins associated with a trithorax-related SET domain protein. Proceedings of the National Academy of Sciences of the United States of America *98*, 12902-12907.

Muniyappa, K., Kshirsagar, R., and Ghodke, I. (2014). The HORMA domain: an evolutionarily conserved domain discovered in chromatin-associated proteins, has unanticipated diverse functions. Gene *545*, 194-197.

Nagy, P.L., Griesenbeck, J., Kornberg, R.D., and Cleary, M.L. (2002). A trithorax-group complex purified from Saccharomyces cerevisiae is required for methylation of histone H3. Proceedings of the National Academy of Sciences of the United States of America *99*, 90-94.

Nezi, L., Rancati, G., De Antoni, A., Pasqualato, S., Piatti, S., and Musacchio, A. (2006). Accumulation of Mad2-Cdc20 complex during spindle checkpoint activation requires binding of open and closed conformers of Mad2 in Saccharomyces cerevisiae. The Journal of Cell Biology *174*, 39-51.

Nislow, C., Ray, E., and Pillus, L. (1997). SET1, a yeast member of the trithorax family, functions in transcriptional silencing and diverse cellular processes. Mol Biol Cell *8*, 2421-2436.

Paull, T.T., and Gellert, M. (1998). The 3' to 5' exonuclease activity of Mre 11 facilitates repair of DNA double-strand breaks. Molecular Cell *1*, 969-979.

Prakash, S., Johnson, R.E., and Prakash, L. (2005). Eukaryotic translesion synthesis DNA polymerases: specificity of structure and function. Annual Review of Biochemistry *74*, 317-353.

Pryde, F., Jain, D., Kerr, A., Curley, R., Mariotti, F.R., and Vogelauer, M. (2009). H3 k36 methylation helps determine the timing of cdc45 association with replication origins. PloS One *4*, e5882.

Pui, C.H., Behm, F.G., Downing, J.R., Hancock, M.L., Shurtleff, S.A., Ribeiro, R.C., Head, D.R., Mahmoud, H.H., Sandlund, J.T., Furman, W.L.*, et al.* (1994). 11q23/MLL rearrangement confers a poor prognosis in infants with acute lymphoblastic leukemia. J Clin Oncol *12*, 909-915.

Rao, B., Shibata, Y., Strahl, B.D., and Lieb, J.D. (2005). Dimethylation of histone H3 at lysine 36 demarcates regulatory and nonregulatory chromatin genome-wide. Molecular and Cellular Biology *25*, 9447-9459.

Rieder, C.L., Schultz, A., Cole, R., and Sluder, G. (1994). Anaphase onset in vertebrate somatic cells is controlled by a checkpoint that monitors sister kinetochore attachment to the spindle. The Journal of Cell Biology *127*, 1301-1310.

Rizzardi, L.F., Dorn, E.S., Strahl, B.D., and Cook, J.G. (2012). DNA replication origin function is promoted by H3K4 di-methylation in Saccharomyces cerevisiae. Genetics *192*, 371-384.

Robzyk, K., Recht, J., and Osley, M.A. (2000). Rad6-dependent ubiquitination of histone H2B in yeast. Science *287*, 501-504.

Santos-Rosa, H., Schneider, R., Bannister, A.J., Sherriff, J., Bernstein, B.E., Emre, N.C., Schreiber, S.L., Mellor, J., and Kouzarides, T. (2002). Active genes are tri-methylated at K4 of histone H3. Nature *419*, 407-411.

Schvartzman, J.M., Duijf, P.H., Sotillo, R., Coker, C., and Benezra, R. (2011). Mad2 is a critical mediator of the chromosome instability observed upon Rb and p53 pathway inhibition. Cancer Cell *19*, 701-714.

Seol, J.H., Kim, H.J., Yang, Y.J., Kim, S.T., Youn, H.D., Han, J.W., Lee, H.W., and Cho, E.J. (2006). Different roles of histone H3 lysine 4 methylation in chromatin maintenance. Biochemical and Biophysical Research Communications *349*, 463-470.

Sethi, N., Monteagudo, M.C., Koshland, D., Hogan, E., and Burke, D.J. (1991). The CDC20 gene product of Saccharomyces cerevisiae, a beta-transducin homolog, is required for a subset of microtubule-dependent cellular processes. Molecular and Cellular Biology *11*, 5592-5602.

Shahbazian, M.D., Zhang, K., and Grunstein, M. (2005). Histone H2B ubiquitylation controls processive methylation but not monomethylation by Dot1 and Set1. Molecular Cell *19*, 271-277.

Shema, E., Tirosh, I., Aylon, Y., Huang, J., Ye, C., Moskovits, N., Raver-Shapira, N., Minsky, N., Pirngruber, J., Tarcic, G.*, et al.* (2008). The histone H2B-specific ubiquitin ligase RNF20/hBRE1 acts as a putative tumor suppressor through selective regulation of gene expression. Genes & Development *22*, 2664-2676.

Shi, X., Hong, T., Walter, K.L., Ewalt, M., Michishita, E., Hung, T., Carney, D., Pena, P., Lan, F., Kaadige, M.R.*, et al.* (2006). ING2 PHD domain links histone H3 lysine 4 methylation to active gene repression. Nature *442*, 96-99.

Shilatifard, A. (2012). The COMPASS family of histone H3K4 methylases: mechanisms of regulation in development and disease pathogenesis. Annual Review of Biochemistry *81*, 65-95.

Simpson, R.T. (1990). Nucleosome positioning can affect the function of a cis-acting DNA element in vivo. Nature *343*, 387-389.

Sironi, L., Mapelli, M., Knapp, S., De Antoni, A., Jeang, K.T., and Musacchio, A. (2002). Crystal structure of the tetrameric Mad1-Mad2 core complex: implications of a 'safety belt' binding mechanism for the spindle checkpoint. The EMBO Journal *21*, 2496-2506.

Smerdon, M.J., and Lieberman, M.W. (1978). Nucleosome rearrangement in human chromatin during UV-induced DNA- reapir synthesis. Proceedings of the National Academy of Sciences of the United States of America *75*, 4238-4241.

Sollier, J., Lin, W., Soustelle, C., Suhre, K., Nicolas, A., Geli, V., and de La Roche Saint-Andre, C. (2004). Set1 is required for meiotic S-phase onset, double-strand break formation and middle gene expression. EMBO J *23*, 1957-1967.

Strahl, B.D., and Allis, C.D. (2000). The language of covalent histone modifications. Nature *403*, 41-45.

Suka, N., Suka, Y., Carmen, A.A., Wu, J., and Grunstein, M. (2001). Highly specific antibodies determine histone acetylation site usage in yeast heterochromatin and euchromatin. Molecular Cell *8*, 473-479.

Sun, Z.W., and Allis, C.D. (2002). Ubiquitination of histone H2B regulates H3 methylation and gene silencing in yeast. Nature *418*, 104-108.

Thorne, A.W., Sautiere, P., Briand, G., and Crane-Robinson, C. (1987). The structure of ubiquitinated histone H2B. The EMBO Journal *6*, 1005-1010.

Unnikrishnan, A., Gafken, P.R., and Tsukiyama, T. (2010). Dynamic changes in histone acetylation regulate origins of DNA replication. Nature Structural & Molecular Biology *17*, 430-437.

v

an Attikum, H., Fritsch, O., and Gasser, S.M. (2007). Distinct roles for SWR1 and INO80 chromatin remodeling complexes at chromosomal double-strand breaks. The EMBO Journal *26*, 4113-4125.

van Attikum, H., Fritsch, O., Hohn, B., and Gasser, S.M. (2004). Recruitment of the INO80 complex by H2A phosphorylation links ATP-dependent chromatin remodeling with DNA double-strand break repair. Cell *119*, 777-788.

Varambally, S., Yu, J., Laxman, B., Rhodes, D.R., Mehra, R., Tomlins, S.A., Shah, R.B., Chandran, U., Monzon, F.A., Becich, M.J.*, et al.* (2005). Integrative genomic and proteomic analysis of prostate cancer reveals signatures of metastatic progression. Cancer Cell *8*, 393-406.

Wang, Y., Reddy, B., Thompson, J., Wang, H., Noma, K., Yates, J.R., 3rd, and Jia, S. (2009). Regulation of Set9-mediated H4K20 methylation by a PWWP domain protein. Molecular Cell *33*, 428-437.

Watkins, J., Weekes, D., Shah, V., Gazinska, P., Joshi, S., Sidhu, B., Gillett, C., Pinder, S., Vanoli, F., Jasin, M.*, et al.* (2015). Genomic Complexity Profiling Reveals That HORMAD1 Overexpression Contributes to Homologous Recombination Deficiency in Triple-Negative Breast Cancers. Cancer Discovery *5*, 488-505.

Winkler, G.S., Kristjuhan, A., Erdjument-Bromage, H., Tempst, P., and Svejstrup, J.Q. (2002). Elongator is a histone H3 and H4 acetyltransferase important for normal histone acetylation levels in vivo. Proceedings of the National Academy of Sciences of the United States of America *99*, 3517-3522.

Wood, A., Krogan, N.J., Dover, J., Schneider, J., Heidt, J., Boateng, M.A., Dean, K., Golshani, A., Zhang, Y., Greenblatt, J.F.*, et al.* (2003). Bre1, an E3 ubiquitin ligase required for recruitment and substrate selection of Rad6 at a promoter. Molecular Cell *11*, 267-274.

Wysocka, J., Swigut, T., Milne, T.A., Dou, Y., Zhang, X., Burlingame, A.L., Roeder, R.G., Brivanlou, A.H., and Allis, C.D. (2005). WDR5 associates with histone H3 methylated at K4 and is essential for H3 K4 methylation and vertebrate development. Cell *121*, 859-872.

Xia, G., Luo, X., Habu, T., Rizo, J., Matsumoto, T., and Yu, H. (2004). Conformation-specific binding of p31(comet) antagonizes the function of Mad2 in the spindle checkpoint. The EMBO Journal *23*, 3133-3143.

Xu, G., Chapman, J.R., Brandsma, I., Yuan, J., Mistrik, M., Bouwman, P., Bartkova, J., Gogola, E., Warmerdam, D., Barazas, M.*, et al.* (2015). REV7 counteracts DNA double-strand break resection and affects PARP inhibition. Nature *521*, 541-544.

Yu, Y., Teng, Y., Liu, H., Reed, S.H., and Waters, R. (2005). UV irradiation stimulates histone acetylation and chromatin remodeling at a repressed yeast locus. Proceedings of the National Academy of Sciences of the United States of America *102*, 8650-8655.

Yuan, G.C., Liu, Y.J., Dion, M.F., Slack, M.D., Wu, L.F., Altschuler, S.J., and Rando, O.J. (2005). Genome-scale identification of nucleosome positions in S. cerevisiae. Science *309*, 626-630.

Zeleznik-Le, N.J., Harden, A.M., and Rowley, J.D. (1994). 11q23 translocations split the "AT-hook" cruciform DNA-binding region and the transcriptional repression domain from the activation domain of the mixed-lineage leukemia (MLL) gene. Proceedings of the National Academy of Sciences of the United States of America *91*, 10610-10614.

Zhang, K., Lin, W., Latham, J.A., Riefler, G.M., Schumacher, J.M., Chan, C., Tatchell, K., Hawke, D.H., Kobayashi, R., and Dent, S.Y. (2005). The Set1 methyltransferase opposes Ipl1 aurora kinase functions in chromosome segregation. Cell *122*, 723-734.

Vita

Andria Schibler was born on January 21st 1983 to Stephanie and Bruce Schibler. She grew up in Dayton, Ohio along side her two brothers Mathew and Michael Schibler and later moved to Springfield, Ohio where she attended Kenton Ridge High School. There she received her first academic successes by being voted (in a peer awarded process), homecoming princess of the sophomore class in 1998, homecoming court in 2000, as well as “Best Sense of Humor” and “Most Likely to Prematurely Age a Teacher” during the senior superlative award ceremony. While attending high school she also received multiple metric based athletic awards such All-League (2000, 2001), All-Southwest District (2000), All-Clark County (2000), All-News Sun (2000), All-Southwest Ohio Region (2000), and All-Ohio in 2000. She was also voted onto the Regional All-Star team (East, 2000) and inducted into the high school athletic hall of fame in 2001. In addition to softball Andria also played on the volleyball, soccer, cross country, swimming, and basketball team. She received The Ohio High School Basketball Coaches Association Scholarship (2000), Society Silver Certificate Award (2000) and was voted as team captain for multiple teams (in a peer elected process).

Lastly, Andria received the Golden Paw Award (2000), was a member of the Spanish National Honor Society (2000), participated as a Student Council Class Representative (Treasurer-2000, President-2001). She was elected as a QUEST mentor and SAAD (Students Against Destructive Decisions) participant.

After high school graduation, Andria attended college at Suffolk University, in Boston, Massachusetts where she played on the varsity softball team and was awarded Rookie of the Year in 2002. She also received acclaim in 2004 where she was ranked 5th in the nation for RBIs per game and 4th in the nation for triples per game during the regular season. Final rankings include 12th in the nation for RBIs per game, 11th in the nation for Triples per game, and she was ranked 21st in the nation for Toughest to Strike Out. She later received her Bachelors of Arts in Biology in 2006.

Between undergraduate studies Andria worked at Harvard Medical School/MEEI, under the supervision of Jarema Malicki, Ph.D. before attending the Graduate School of Biomedical Sciences (GSBS) at the University of Texas M.D. Anderson Cancer Center, in Houston, Texas in August of 2007.

Upon entering graduate School, Andria joined the lab of Dr. Sharon Dent in the spring of 2008. She has received multiple awards while attending GSBS including the Genes and Development Precandidacy Poster Award (2010), the Schissler Fellowship (2011), the Genes and Development Retreat Presentation Award (1st place, 2011), the Graduate Student Retreat Postcandidacy Poster Award (2nd place, 2012), the Andrew Sowell-Wade Huggins Scholarship (2013) and selected as a CPRIT Graduate Scholar (2014). She was also elected as a Graduate Student Association Representative (2012).

During her time in the Malicki and Dent lab, Andria has also contributed to a number of academic publications as listed here:

1) Lan X, Koutelou E, Schibler AC, Chen YC, Grant P, Dent SY. PolyQ expansions in ATXN7 affect solubility but not activity of the SAGA deubiquitinating module. Mol Cell Biol. May 2015.

2) Tomida J, Takata K, Lange S, Schibler AC; Yousefzadeh M, Bhetawal S, Dent SY, Wood R. REV7 is essential for DNA damage tolerance via two REV3L binding sites in mammalian DNA polymerase **ζ**. NAR. January 2015.

3) Butler JS, Koutelou E, Schibler AC, Dent SY. Histone-modifying enzymes: regulators of developmental decisions and drivers of human disease. Epigenomics. April 2012.

4) Wilson MA, Koutelou E, Hirsch C, Akdemir K, Schibler A, Barton MC, and Dent SY. Ubp8 and SAGA regulate Snf1 AMP Kinase Activity. Mol Cell Biol. August 2011.

5) Schibler A. and Malicki J. A screen for genetic defects of the zebrafish ear. Mech Dev. May 2007.